Contribution of tree fine roots to the silicon cycle in a temperate forest ecosystem developed on three soil types

Marie-Pierre Turpault[1], Christophe Calvaruso[2], Gil Kirchen[1], Paul-Olivier Redon[3], Carine Cochet[1]

[1]UR 1138, INRA "Biogéochimie des Ecosystèmes Forestiers", Centre INRA de Nancy, Champenoux, 54280, France

[2]EcoSustain, Environmental Engineering Office, Research and Development, Kanfen, 57330, France

[3]Andra, Direction de la Recherche et Développement, Centre de Meuse/Haute-Marne, Route départementale 960, Bure, 55290, France

Correspondence to: Marie-Pierre Turpault (marie-pierre.turpault@.inra.fr)

Abstract

The role of forest vegetation in the silicon (Si) cycle has been widely examined. However, to date, rare is known about the specific role of fine roots. The main objectives of our study were to assess the influence of fine roots on the Si cycle in a temperate forest in northeastern France. Silicon pools and fluxes in vegetal solid and solution phases were quantified within each ecosystem compartment, i.e., the atmosphere, aboveground and belowground tree tissues, forest floor, and different soil horizons, on three plots, each with different soil types, i.e., Dystric Cambisol (DC), Eutric Cambisol (EC), and Rendzic Leptosol (RL). In this study, we took advantage of a natural soil gradient, from shallow calcic soil to deep moderately acidic soil, with similar climates, atmospheric depositions, species composition and management. Soil solutions were measured monthly for four years to study the seasonal dynamics of Si fluxes. A budget of dissolved Si was also determined for the forest floor and soil layers. Our study highlighted the major role of fine roots in the Si cycle in forest ecosystems for all soil types. Because of the abundance of fine roots mainly in the superficial soil horizons, their high Si concentration (equivalent to that of leaves and two orders higher than that of coarse roots) and their rapid turnover rate (approximately one year), the mean annual Si fluxes in fine roots in the three plots ranged from 68 to 110 kg ha^{-1} y^{-1} for the RL and the DC, respectively. The turnover of fine roots and leaves was approximately 71% and 28% of the total Si taken up by trees each year, respectively, demonstrating the importance of biological recycling in the Si cycle in forests. Less than 1% of the Si taken up by trees each year accumulated in the perennial tissues. This study also demonstrated the influence of soil type on the concentration of Si in the annual tissues and therefore on the Si fluxes in forests. The concentrations of Si in leaves and fine roots were approximately 1.5-2.0 times higher in the "Si-rich" DC compared to the "Si-poor" RL. In terms of the dissolved Si budget, there were large amounts of dissolved Si in the three plots on the forest floor (9.9 to 12.7 kg ha^{-1} y^{-1}) and in the superficial soil horizon (5.3 to 14.5 kg ha^{-1} y^{-1}), and Si decreased with depth in plot DC (1.7 kg ha^{-1} y^{-1}). The amount of Si leached from the soil profile was relatively low compared to the annual uptake by trees (13% in plot DC to 29% in plot S3). The monthly measurements demonstrated that the seasonal dynamics of the dissolved Si budget were mainly linked to biological activity. Notably, the peak of dissolved Si production in the superficial soil horizon was during the winter and probably resulted from fine root decomposition. Our study reveals that biological processes, particularly those of fine roots, play a predominant role in the Si cycle in temperate forest ecosystems, while the geochemical processes appear to be limited.

1 Introduction

It has recently been shown that intense biogeochemical cycling of Si occurs in the different terrestrial ecosystems, i.e., wetlands (Struyf et al., 2007; Emsens et al., 2016), grasslands (Blecker et al., 2006; White et al., 2012), tropical forests (Lucas et al., 1993, Alexandre et al., 1997) and temperate forests (Bartoli, 1983; Watteau and Villemin, 2001; Gerard et al, 2008; Cornelis et al., 2010a; Cornelis et al., 2011a; Sommer et al., 2006; Sommer et al., 2013). Several review papers well described that soil DSi is taken up by vascular plants and translocated into biogenic Si (BSi) under opal form which is deposited into the cell walls, cell luminas and intercellular spaces (Jones and Handreck, 1965; Conley et al., 2002; Cornelis et al, 2011b; Struyf and Conley, 2012). These structures are called phytoliths. Other important producers of biogenic Si are animals especially diatoms, sponges and testate amoebae. (Struyf and Conley, 2012; Sommers et al., 2006; Puppe et al., 2014; Puppe et al., 2015).

According to Conley (2002), the annual fixation of DSi into terrestrial ecosystems has been estimated to range from 60 to 200 Tmoles. That represents 10 to 40 times more than yearly export DSi and suspended biogenic Si from the terrestrial geobiosphere to the coastal zone (Conley, 2002). Vegetation can thus be considered as a factory of BSi which returns to the soil as organic matter through biological recycling. Because BSi in general is more soluble than silicate minerals, BSi strongly contributes to the DSi pool (Fraysse et al., 2009 ; Cornelis and Delvaux, 2016).

Based on the assumption that the storage of Si is limited in roots (Bartoli and Souchier, 1986) and because fine root sampling and cleaning before analyses are long and tedious processes, studies in forest ecosystems mainly focus on the importance of litterfall recycling on the Si biogeochemical cycle without quantifying Si in the roots (Gérard et al., 2008; Cornelis et al., 2010a; Sommer et al., 2013).

However, Krieger et al (2017) recently showed that Si in deciduous trees (European beech, *Fagus sylvatica* and sycamore maple, *Acer pseudoplatanus*) generally precipitates as a thin layer (< 0.5 µm) around the cells, especially in roots and bark. These small-scale phytogenic Si was demonstrated to influence various soil and plant processes (Meunier et al., 2017 ; Puppe et al., 2017).

Considering the large amount of Si precipitates in roots (Krieger et al., 2017) and the rapid turnover of fine roots in forest ecosystems (approximately one year in beech forests in Europe; Brunner et al., 2013), we hypothesized that fine roots could significantly contribute to the input of BSi into the soil.

To test this hypothesis, we quantified during a four-year observation period (i) the total and annual accumulations of Si in stand belowground and abovegound biomasses while distinguishing annual and perennial compartments, ii) the Si input fluxes in the forest floor (litterfall and small woods, aboveground exploitation residues) and in the soil (fine roots and belowground exploitation residues). The study was led in a lowland (low lateral transfer of material) deciduous temperate forest developed on three soils, ranging from a shallow calcic soil to a deep acidic soil, with mull to acid mull humus. These humus forms quickly degrades, contain few soil particles and no root thus allowing to determine the DSi issued from the degradation of organic layers contrary to mor or moder humus forms (Sommer et al., 2006; Cornelis et al., 2010a). In addition, we monthly quantified in these ecosystems the Dsi inputs and outputs, i.e., rainfall, foliar leaching and drainage, in order to assess the seasonal dynamics of these fluxes induced by biological activities.

2 Materials and Methods

2.1 Experimental site

The experimental site, hereafter referred to as the Montiers site (http://www.nancy.inra.fr/en/Outils-et-Ressources/montiers-ecosystem-research), is located in the Montiers-sur-Saulx beech forest in northeastern France (Meuse, France, latitude 48° 31' 54'' N, longitude 5° 16' 08'' E). The site is 73 ha and has been managed jointly by the INRA-BEF (French National Institute for Agricultural Research – Biogeochemical cycles in Forest Ecosystems research unit) and by the ANDRA (French National Radioactive Waste Management Agency) since 2012. The different steps of site establishment are described in detail in Calvaruso et al. (2017). The Montiers site is part of different national and international research networks, i.e., SOERE (Long-lasting observation and experimentation for the research on environment)-OPE (Perennial Environment Observatory; http://www.andra.fr/ope/index.php?lang=en&Itemid=127) and F-ORE-T (Functioning of Forest Ecosystems; http://www.gip-ecofor.org/f-ore-t/), and AnaEE (Analysis and Experimentations on Ecosystems; https://www.anaee.com/). The mean annual rainfall and temperature over the last twenty years were 1069 mm and 9.8°C, respectively (calculated from Météo-France data). The geology of the Montiers site consists of two overlapping soil parent materials: an underlying Tithonian limestone surmounted by detrital acidic Valanginian sediments. The calcareous bedrock contains mainly calcium carbonate and ~3.4% clay minerals. The overlying detrital sediments are complex, as they result from various depositions and are composed of silt, clay, coarse sand and iron oxide nodules (for more details, see Calvaruso et al., 2017). The site is covered by a homogeneous, same-aged stand (approximately 50 years old in 2010) with the same management approaches. The stand was mainly composed of beech (89%) and 11% of other deciduous species, i.e., sycamore maple (*Acer pseudoplatanus*), ash (*Fraxinus excelsior*), pedunculate oak (*Quercus robur* L.), European hornbeam (*Carpinus betulus* L.), and wild cherry (*Prunus avium*). The site was also composed of three different soil types, i.e., Dystric Cambisol (DC), Eutric Cambisol (EC), and Rendzic Leptosol (RL) (FAO, 2016). A schematic representation of the soil profiles and their location are presented in Kirchen et al. (2017). Table 1 presents the main characteristics of these different soil types, ranging from acidic and deep soils to calcic and superficial soils, developed on acidic Valanginian and detritic sediments and Portlandian limestone, respectively. Humus type is a eutrophic mull for the RL and EC and an acidic mull for the DC.

Three experimental plots were built on the three different soils to monitor water and element fluxes as well as tree growth, over four years. Each plot was composed of three subplots (replicates), equipped with the same monitoring devices designed for the sampling of aboveground and belowground solutions at different depths, soil at different depths, organic horizons, litterfall, and four subplots equipped for standing aboveground and belowground biomasses as well as tree growth. In addition, a 45-m high flux tower was placed within the site (close to plot DC) to collect rainfall and atmospheric deposits.

2.2 Sampling

2.2.1 Solutions and dust deposits

Solutions and dust deposits were sampled every four weeks between January 2012 and December 2015, representing four years of monitoring.

Rainfall was collected on top of the flux tower by three polyethylene collectors (0.24 m^2 opening) to obtain dust deposition. The procedure of dust deposit sampling is described in Lequy et al. (2014). Briefly, rainfall was

centrifuged for 40 minutes at 3500 tr.min^{-1} to separate the solid phase from the solution (the solid phase consists of the dust deposits). Rainfall volumes were obtained from a Météo-France weather station located in Biencourt-sur-Orge (Meuse, France), which is 4.3 km from the Montiers site.

The throughfall was collected in each replicate by 4 polyethylene gutters (0.39 m^2 opening), placed 1.2 m above the forest ground.

The stemflow was collected in each replicate on 6 trees of different sizes, using polyethylene collars attached horizontally to the stem at 1.50 m. Trees were chosen to cover most of the range of stem circumferences at 130 cm height (C130) in each plot. To prevent the solution from freezing, the stemflow was collected in underground storage containers during the winter.

The gravitational soil solutions (zero-tension lysimeters, ZTL) were collected beneath the forest floor and at different soil depths, -10 and -30 cm (in DC, EC and S3), -60 cm (in DC and EC) and -90 cm (in DC), with large plate lysimeters (40 cm * 30 cm, 0.12 m^2; 3 repetitions per soil depth and per replicate) or thin rod-like lysimeters (0.07 m^2; in clusters of 8; 3 repetitions per soil depth and per replicate).

The bound soil solutions (tension lysimeters, TL) were collected by ceramic cups inserted in the soil at different depths, -10 and -30 cm (in DC, EC and S3), -60 cm (in DC and EC) and -90 cm (in DC), with 4 repetitions per depth and per replicate. These ceramic cups were connected to an electric vacuum pump that maintained a constant depression between -0.5 and -0.6 bar.

2.2.2 Tree compartments

Three beech trees were harvested in each plot in 2009 to collect stem wood and bark and branches. Subsequently, the branches latter were separated into different classes, i.e., < 4, 4-7 and > 7 cm in diameter, according to Henry et al. (2011). The detailed procedure for collecting stem wood and bark and branches is described in Calvaruso et al. (2017).

The fine roots (< 2 mm diameter) were collected during March-April 2011 in three soil pits (approximately 0.4 m wide) for each replicate, where the soil material was cut and extracted by layer (0-5, 5-15, 15-30, 30-45, 45-60 cm, and 60-90 cm, when possible). A two-step procedure was applied to accurately assess the fine root biomass (Bakker et al., 2008), without having to transport soil to the laboratory. The first step involved collecting, *in situ*, the fine roots from the block of soil extracted from each soil layer. Then, a part of the soil block (approximately 2 kg) was collected. The second step, at the laboratory, consisted of using a tweezer to collect all the remaining fine roots in this soil aliquot. This second step allowed for the assessment of the fraction of fine roots uncollected during the first step. The fine roots collected during the two steps were washed at the laboratory, dried in a stream air-drier for three days and then weighed. For each layer, the total biomass of fine roots was obtained by summing the fine root biomass collected during the first step and the fine root biomass collected during the second step, multiplied by the ratio total soil block mass / soil aliquot mass. Roots with a diameter > 2 cm (small and coarse roots) were collected in February 2017 in three soil pits (approximately 0.4 m wide) for each plot where soil material was cut and extracted at approximately 20 cm depth. This method does not allow quantification of small and coarse root biomass, which were determined through allometric equations (Le Goff and Ottorini, 2001). An aliquot of each root sample (fine, small and coarse) was then collected to determine element concentration. Each aliquot was carefully washed under a binocular microscope with distilled water, using tweezers and an ultrasound

gun. The absence of soil particles was carefully checked under a binocular microscope with a magnification of 10x. The operation was repeated until all soil particles were removed to prevent soil pollution in the root analyses.

The litterfall was collected in 6 litter traps (0.34 m^2 each) per replicate. The litter was harvested seven times per year, avoiding litter degradation in the litter traps. During the harvest, the litter was separated into three compartments, i.e., (i) leaves and (ii) buds, beechnuts, fruit capsules (annual compartments), and (iii) small branches falling from the trees (perennial compartment). The leaves, buds, beechnuts, and fruit capsules belong to annual tree compartments (recycling each year) while small branches belong to perennial compartments.

2.2.3 Forest floor

We defined the forest floor by the set of organic horizons (Oln, Olv, Of and Oh) above the organo-mineral horizon (Ah), and the small dead wood at the soil surface.

Organic horizons were collected in June 2010 in a calibrated metal frame (surface area of 0.1 m^2). Nine samples were collected in each replicate. Because the lower organic horizons were in direct contact with the superficial soil horizon, it was very difficult to sample them without soil contamination. The presence of soil particles, very rich in Si, mixed with the organic horizons, can induce a drastic overestimation of the Si pool in this compartment. As a result, we decided to carefully sample, on site, six organic horizon samples without the fraction contacting the soil, called “pure organic horizons”. These “pure organic horizons” were used to determine the soil fraction in the organic horizon collected on the three plots (see the method in part 2.4.2).

Small dead wood from the previous thinning (winter 2009-2010) was harvested in June 2010 at the three stations in a calibrated metal frame (surface area of 0.6084 m^2). Nine samples were collected in each replicate, according to a grid.

2.2.4 Soil

Nine soil samples were collected in June 2010 in each replicate, along a 15 x 15 m grid. At each point, samples were extracted through an auger, by layer, 0-5, 5-15, 15-30, 30-45, and 45-60 cm, and 60-90 cm when possible.

2.3 Analytical methods

2.3.1 Si content in solutions

Solutions of rainwater, stemflow, throughfall, forest floor and soil were filtered at 0.45 µm, stored at 4°C and analysed during the week following the sampling. The Si content in the solutions was measured by inductively coupled plasma-atomic emission spectrometry (ICP-AES Agilent Technologies 700 type ICP-OES, Santa Clara, USA).

2.3.2 Si content in biomass

Samples from the aboveground and belowground compartments of the trees, litterfall and forest floor were dried in a stream air-drier (at 65°C), then ground and encapsulated for analysis. The total Si content in the biomass was assessed by X fluorescence, using an X Fluorescence sequential spectrometer S8 TIGER 1kW (Bruker, Marne la vallée, France).

2.3.3 Si content in soil and dust deposits

The total Si content in soil organo-mineral and mineral layers (preliminarily sieved at 2 mm) and in dust deposits were determined by inductively coupled plasma-atomic emission spectrometry (700 Series ICP-OES, AGILENT TECHNOLOGIES) after alkaline fusion in $LiBO_2$ and in HNO_3.

2.3.4 Microscopic analysis

Samples of fine roots, stem and branch bark, fruit capsules, bud scales and fresh and altered leaves (from organic horizons) of beech tree samples were mounted on glass plates, using double-coated carbon conductive tabs and covered with carbon. The samples were examined at the GeoRessources laboratory (University of Lorraine) for biomineral occurrence and composition, using a Hitachi S-4800 scanning electron microscope (SEM) equipped with an energy-dispersive X-ray spectrometer (EDX), containing a lithium-drifted Si detector. The SEM analyses were carried out using an acceleration voltage of 10 or 15 kV.

2.4 Calculation of Si pools and fluxes in solutions and solids

In each plot, Si fluxes and pools were obtained by multiplying the amount of solution or solid by the concentration of Si in the given compartment. All monthly Si fluxes were calculated on a one-hectare basis and were summed over calendar years to compute the annual fluxes. The dissolved Si budget was also calculated for forest floor and soil layers by the difference between input and output fluxes.

In the following sections (2.4.1 to 2.4.10), we will only present the Si fluxes or pools for which the method of calculation differs from the calculation of multiplying the amount of solution or solid by the concentration of Si in the compartment.

2.4.1 Dust deposits

To take into account the loss of particles during the collection of dust deposits from rainfall, a test using standard minerals was done to assess the efficiency of the procedure (Lequy et al., 2014). The efficiency was estimated at 72%. Thus, the total weight of dust deposits per year was determined as the weight of dust deposits collected on site, divided by a correction factor of 0.72.

2.4.2 Organic horizons

The percentage of soil mixed with the organic horizons was determined through the use of titanium (Ti). This element is a good tracer of soil pollution in the collected organic horizons because Ti is in very low abundance in pure organic horizons (< 0.3 mg kg-1), while it is more abundant in soils (> 4 mg kg^{-1}). We measured Ti content in the soil surface layer (0-5 cm), in the pure organic horizons and in the organic horizons collected on the three plots. The percentage of soil in the organic horizons was assessed following Eq. (1):

$$\text{Soil \%} = [(Ti_{Hb} - Ti_{Hp}) / (Ti_S - Ti_{Hp})] \quad (1)$$

where Ti_{Hb} is the concentration of Ti in the organic horizons, Ti_{Hp} is the concentration of Ti in the pure organic horizons, and Ti_S is the mean concentration of Ti in the 0-5 cm horizon of soil for each plot. The mean soil fraction

represented less than five percent of the total organic horizon mass in our study. The fraction of Si brought by soil contamination was deducted to obtain the Si content in the organic horizons.

2.4.3 Stemflow and stand deposition

To transform the stemflow volumes to a water flux, C130 was assumed to explain the inter-individual stemflow volume variability within a species. Thus, all the trees in each plot were separated into several C130 classes, and the correlation between the stemflow volume and the C130 was verified for the entire sampling period. Using a trend line equation, a mean monthly stemflow volume was then assigned to each C130 class. The stemflow at the plot scale for a given C130 class (SF_z; in mm) is given by following Eq. (2):

$$SF_z = V_z \cdot \left(\frac{N_z}{A}\right) \quad (2)$$

where z is the C130 class, V_z is the mean stemflow volume per tree in the given C130 class (in l), N_z is the number of trees in the given C130 class and A is the plot area (in m^2). Total stemflow at the plot scale was obtained by summing the stemflow fluxes of all C130 classes.

The Si stand deposition, i.e., the amount of Si (kg ha^{-1} y^{-1}) reaching the soil after crossing over the canopy, was determined as the sum of the Si fluxes in throughfall and stemflow.

2.4.4 Drainage flux

The BILJOU© model (Granier et al., 1999) was applied in the three plots at the Montiers site to assess the water drainage flux for the different soil layers. The detailed procedure and the data are presented in Kirchen et al. (2017). The gravitational water flux was determined for each soil layer and date from the collected gravitational volume. The bound water flux was obtained by subtracting the water gravitational flux from the modelled water drainage flux. In this study, we determined that the water gravitational flux/water bound flux ratio was approximately 80/20, which is similar to the measurement from a Cl tracer in a beech temperate forest in Fougères in Legout et al. (2009).

Thus, the monthly elements drainage fluxes were calculated at each depth following Eq. (3):

$$D_{Si} = D_G \times C_{SiG} + D_B \times C_{SiB} \quad (3)$$

where D_{Si} is the drainage flux of Si, D_G is the water drainage via rapid gravitational transfer, C_{SiG} is the concentration of Si in the gravitational soil solution collected by zero-tension lysimeters, D_B is the water drainage via slow bound transfer, and C_{SiB} is the concentration of Si in the bound soil solution collected by ceramic cups.

The element mass balances were calculated for the following soil layers, according to the installation depths of the lysimeters in the three plots: forest floor (FF), from the forest floor to -10 cm (soil layer L1), between -10 and -30 cm (L2), between -30 and -60 cm (L3) and between -60 and -90 cm (L4). For each soil layer, the mass balance of the elements was calculated as the difference between the drainage at the bottom of the layer and the drainage entering the layer (Eq. 4):

$$MB_{Si} = D_{Si2} - D_{Si1} \quad (4)$$

where MB_{Si} is the mass balance of Si in a given soil layer, D_{Si1} is the incoming drainage flux of Si and D_{Si2} is the drainage flux at the bottom of the soil layer.

2.4.5 Aboveground tree biomass

The evaluation of aboveground tree biomass was calculated according to procedures described in Saint-André et al. (2005). It included four steps, (i) the circumference of all trees was measured at 1.30 m height, C_{130}, in 2011 and 2015; (ii) eight trees in each plot, representing the range of C_{130}, stem bark and wood and 0-4, 4-7 and > 7 cm diameter branches were sampled; (iii) the weighed allometric equations fitted for each ecosystem compartment were calculated according to Calvaruso et al. (2017); and (iv) tree biomass (stem bark and wood and 0-4, 4-7 and > 7 cm diameter branches) was quantified per hectare by applying fitted equations to the stand inventories. Annual aboveground biomass production and Si immobilization in aboveground biomass were calculated as the difference between the biomass or Si amount in the biomass calculated for 2015 and 2011, divided by four.

2.4.6 Fine root flux

The fine root turnover rate is dependent on the fine root biomass and the annual production but also on the various methods and calculations used to determine the rate (Jourdan et al., 2008; Gaul et al., 2009; Finer et al., 2011; Yuan and Chen, 2010). In this study, the annual fine root production was calculated by using the mean fine root turnover rate of 1.11±0.21 y^{-1}, issued from the last available European data compilation for beech forests (Brunner et al., 2013). The turnover rate corresponds to the ratio between the production of fine roots during the growing season and the mean biomass of living fine roots during the year. The Si flux from fine roots was calculated by multiplying the annual fine root production by the Si concentration in the fine roots.

2.4.7 Small and coarse roots

The small and coarse root biomass as well as the annual root increment were determined using allometric equations, linking the stem diameter at breast level and root biomass of beech trees (Le Goff and Ottorini, 2001). The pools and fluxes of Si in small and coarse roots were calculated by multiplying the total biomass or the annual root increment by the Si concentration in small and coarse roots.

2.4.8 Exploitation residuals and harvest

To take into account the influence of forestry practices after 2010 on the Si cycle, we simulated a stand thinning based on the forestry practices applied in the Montiers massif by the French National Forestry Office. At this stage of stand development, the National Forestry Office carries out a thinning every seven years, with an aboveground biomass cut of approximately 40 t ha^{-1}. Because the amount of biomass cut is dependent on the stand aboveground biomass, we integrated this parameter into our calculation of exploitation residuals and harvest.

We determined that the aboveground biomass that will be cut during the next thinning (winter 2017-2018) will be approximately 40.0, 44.3, and 35.0 t ha^{-1} in plots DC, EC, and RL, respectively. The root biomass remaining from this thinning will represent approximately 7.9, 9.6, and 6.9 t ha^{-1} in plots DC, EC, and RL, respectively.

From the data regarding the proportion of the different tree compartments in the total aboveground biomass at the Montiers site (stem wood and bark, < 4 cm, 4-7 cm and > 7 cm diameter branches; Calvaruso et al. 2017), we determined the biomass of residuals (< 4 cm, and 4-7 cm diameter branches) and exports (> 7 cm diameter branches, stem wood and bark) issued from this thinning for each station. The roots were not exported.

Because thinning in this region is generally done every seven years, we obtained the annual Si amounts restituted to the soil and exported by dividing the total exploitation residuals by seven.

2.4.9 Foliar leaching

The amount of Si released in foliar leachates throughout the year (Si_{FL}, in kg Si bha^{-1} y^{-1}) was assessed following Eq. 5:

$$Si_{FL} = Si_{SD} - Si_{R} \quad (5)$$

where Si_{SD} is the amount of Si in the stand deposition throughout the year, and Si_{R} is the amount of Si in annual rainfall. All these parameters are assessed in kg Si ha^{-1} y^{-1}.

2.4.10 Tree uptake

The amount of Si taken up by trees throughout the year (Si_{Up}, in kg of Si by ha^{-1} y^{-1}) was assessed following Eq. 6:

$$Si_{Up} = Si_{I_{AG}} + Si_{I_{BG}} + Si_{R_{FL}} \quad (6)$$

where $Si_{I_{AG}}$ is the amount of Si immobilized in the total aboveground biomass of trees (stem bark and wood, branches, leaves and buds, beechnuts and fruit capsules) throughout the year, $Si_{I_{BG}}$ is the amount of Si immobilized in the total belowground biomass of trees (coarse, small and fine roots) throughout the year, and $Si_{R_{FL}}$ is the amount of Si released in foliar leachates throughout the year. All these parameters were assessed in kg Siha^{-1} y^{-1}.

2.5 Statistical analysis

The descriptive statistical parameters (e.g., mean, standard deviation, variation coefficient) were performed using XLSTAT 2017 software. The normality of the distribution was checked, using the Shapiro-Wilk test. As our data did not follow a normal distribution, the non-parametrical Kruskal-Wallis test was performed to compare the different soil types, biomass pools, biomass increments, Si content, Si pools, and Si fluxes for each tree compartment, and the total soil Si at the threshold level of 0.05. The post hoc Bonferroni correction was used for the pairwise comparison. We used the R version 3.3.1 statistical software (R Development Core Team, 2016) and specifically, the R package nlme to test the effect of soil type on annual Si fluxes, by means of a mixed linear analysis of variance (ANOVA) with soil type and their interaction as fixed effects. The significance of differences in element content between the gravitational and bound solutions and between plots was tested by the Student's t-test. Confidence intervals were established at the 0.05 probability level for all statistical tests.

3 Results

3.1 Si in solids

3.1.1 Microscopic observations of Si deposits in vegetation and the forest floor

In fresh leaves, Si precipitates in cell walls but also in intercellular spaces, generally forming Si deposits called phytoliths, which are several micrometres (Figure 1a). In all tree compartments, except wood, these Si deposits mostly occurred as fine coating layers thinner than 0.3 µm in the inner cell walls of fruit capsules (Figure 1b), stem bark (Figures 1d and 1e), bud scales (Figure 1f) and roots (Figures 1g, 1h and 1i). The cells covered with Si deposits were in the external parts of the roots and the branch and stem bark (Figures 1d and 1g). Occasionally, Si was present on cell lumina (Figure 1e).

Aged leaves in the organic horizon were colonized by hyphae and amoebae (Figure 1c) and presented large voids. The Si deposits disappeared from the plant cells but were present in the observed testate amoebae.

3.1.2 Si pools and fluxes in aboveground tree biomass

The calculated standing aboveground biomass in 2011 increased as follows: RL < DC < EC with significant differences between EC and RL (factor 1.4). (Table 2). The stem bark had the highest Si concentration in the three plots, and the Si pool in this compartment represented approximately 40% of the total Si pool in the aboveground tree biomass. The younger the structures were, the higher Si concentration. Small branches were approximately three times more concentrated than coarse branches in the three soils (Table 2). The amount of Si immobilized in the standing aboveground biomass ranged from 20.1 kg ha^{-1} on the RL to 26.2 kg ha^{-1} on the EC. The annual biomass production between 2011 and 2015 increased as follows: RL < EC < DC with significant differences between DC and RL (factor 1.7). As a result, the amount of Si immobilized in the aboveground biomass each year between 2011 and 2015 ranged from 0.98 kg ha^{-1} on the RL to 1.82 kg ha^{-1} on the DC.

3.1.3 Si pools and fluxes in belowground tree biomass

The fine root biomass measured for the entire soil profile was calculated between 7.3 $t.ha^{-1}$ for the DC (90 cm thickness) and 10.6 $t.ha^{-1}$ for the EC (90 cm thickness) (Table 2). However, the fine root density (in t.ha-1 for one cm of soil) in the RL was the higher. Regardless of the soil type, fine root biomass decreased with depth. No significant difference in fine root biomass was observed for any soil layer between the three soils. The concentrations of Si in fine roots were high in the three soils and increased as follows: RL < EC <. The Si pools in the fine roots were important reaching almost 100 kg ha^{-1} in the DC. Based on the turnover rate of fine roots, as determined by Brunner et al. (2013) for beech trees, i.e., 1.11 ± 0.21 y^{-1}, we calculated that the annual Si fluxes resulting from fine root decomposition overpassed 100 kg ha^{-1} in the DC.

The calculated small and coarse root biomass was three times higher than that of the fine roots, representing thus approximately 75% of the total root biomass in the three plots, but the concentrations of Si in coarse roots were two orders of magnitude lower than the concentration in fine roots. As observed for fine roots, the Si concentrations in coarse roots were higher in the DC compared to the RL. The annual immobilization of Si in coarse roots was very low for the three soils and was negligible in comparison to the flux induced by fine root functioning.

3.1.4. Si fluxes in exploitation residues and harvests

The biomass of belowground and aboveground exploitation residues, expressed on an annual basis overpassed2.0 t ha^{-1} y^{-1}(Table 2), with a 1:1 ratio belowground / aboveground. The aboveground exploitation residues were three to six times more concentrated in Si than the belowground ones The amount of Si returning to the soil through exploitation residues was lower than than 0.50 kg ha^{-1} y^{-1}. This value was of very close to the amount of Si exported from the ecosystem through harvests induced by a dynamic forestry practice o the study site.

3.1.5 Si pool in forest floor

In 2010, the forest floor biomass drastically differed between the different soil types, about two times more important on the DC (acid mull) compared to the RL (eutrophic mull). The part of small wood (residuals from the

previous thinning) was higher in the DC compared to the other two soil types, making up approximately 40% and 20% of the total forest floor, respectively (Table 2). The Si pools in the forest floor ranged from about 150 kg ha^{-1} on the RL to about 250 kg ha^{-1} on the DC. Because organic horizons have higher concentrations of Si than small woods, organic horizons represented more than 95% of the Si pools in the forest floor.

3.1.6 Si fluxes in litterfall

The annual litterfall between 2012 and 2015 ranged from 5.2 and 6.0 $t.ha^{-1}$ (Table 2). No significant difference was observed between the three plots, regardless of the tree compartment. Dead leaves represented approximately 70% of the total annual litterfall, while branches and twigs represented 10%, and buds, beechnuts and fruit capsules represented 20%. Regardless of the soil type, the Si content of leaves was higher than the other litterfall compartments, measuring 9-10 times higher than branches/twigs and 2-5 times higher than buds, beechnuts, fruit capsules. Because of their high biomass and Si concentration compared to the other litterfall compartments, leaves were the main fraction of the Si pool (> 90%) in the litterfall in the three plots. Litter leaves collected in DC were twice as concentrated in Si than litter leaves collected in RL (11.3 against 5.6 g kg^{-1}), meaning that the annual Si flux from litterfall was significantly higher on the DC (44.8 kg ha^{-1}) compared to the RL (25.2 kg ha^{-1}).

3.1.7 Si pool in soils and flux of dust deposits

The total Si content and pools in the fine earth fraction were significantly lower in the RL compared to the DC and to the EC (Table 3). The total Si pools in the first 90 cm of soil overpassed $2.4.10^6$ kg ha^{-1} in the DC and EC as opposed to approximately $7.2.10^5$ kg ha^{-1} in the RL.

The dust deposit annual flux between 2012 and 2015, collected on the flux tower of the DC plot above the canopy representing an annual Si input of approximately 6.0 kg ha^{-1} (Table 4).

3.2 Si in solution: Dissolved Si

3.2.1 Si flux in aboveground solutions

The mean annual Si concentration in the rainfall was very low (Table 4) compared to stand deposition (Table 4), representing an annual Si flux of approximately 0.2 kg ha^{-1}. Consequently, the stand deposition and foliar leaching did not significantly differ between the three plots (Table 4). In the three plots, the throughfall solution was enriched in Si (Table 4), and its maximum concentration occurred in during the leafed period, especially during the senescence period (Figure 2). Although the stemflow solution was more concentrated in dissolved Si (Table 4) than the throughfall (Table 4), throughfall contributed a large amount (up to 85%) to the Si stand deposition.

3.2.2 Si fluxes in the forest floor

Over the study period (2012-2015), the solution collected under the forest floor was enriched in Si compared to the aboveground one (approximately one order of magnitude; Table 4) and was equivalent on the three soil types. The net Si production in the forest floor was highest between September and January and was at a minimum in April, particularly in plot RL (Figure 3). The mean annual dissolved

Si production in the forest floor ranged between 12.4 to 9.5 kg ha^{-1} y^{-1} in plots DC and RL, respectively (Table 4).

3.2.3 Si fluxes in the soil profile

Regardless of the soil type, the mean annual dissolved Si concentration generally increased with soil depth for both kinds of solutions, except in the deeper soil layers where the Si concentration remained constant (Figure 4a). The dissolved Si concentrations in the gravitational solution (ZTL) in the 0 to 30 cm soil layers and in the bound-solutions (TL) in the 0-60 cm soil layers increased less than in the forest floor. Regardless of the soil type and depth, the TL solutions were more concentrated in dissolved Si than the ZTL solutions (approximately 1.1 to 1.8 times more; Figure 4a). No matter the depth and the soil type, dissolved Si concentrations in TL solutions showed seasonal variations, with high concentrations between August and December and low concentrations between February and June, which was not the case for ZTL concentrations (Figure 4b). The maximum concentration of dissolved Si did not depend on the drainage fluxes (data not shown).

The Si budget revealed a net annual production of dissolved Si in the 0-10 cm and 10-30 cm layers, ranging from 5.3 kg ha^{-1} y^{1} in plot DC to 14.5 kg ha^{-1} y^{-1} in plot RL and from 2.3 kg ha^{-1} y^{-1} in plot DC to 5.4 kg ha^{-1} y^{-1} in plot EC, respectively (Figure 5). The production of dissolved Si drastically decreased with the depth. In the 60-90 cm layer of plot DC, we even observed a decrease of the amount of dissolved Si (Figure 5), resulting from its immobilization during the autumn (Figure 3). In addition, we observed high seasonal variations of the dissolved Si budget, which were more marked in the top soil layers (Figure 3). The lowest net production in these horizons was between June and August, while the maximum production rates were observed between September and February.

3.3 Si flux taken up by trees

By adding amounts of the Si immobilized each year in the different tree compartments, i.e., perennial aboveground biomass, leaves, bud scales, beechnuts and fruit capsules, small and coarse roots, and fine roots and the foliar leachate, we determined that the annual uptake of Si by the stand was approximately 157, 141, and 95 kg ha^{-1} in plots DC, EC, and RL, respectively.

4 Discussion

4.1 Si accumulation and internal fluxes in trees

Perennial tissues, such as stem, branches and coarse roots, whose biomass represented more than 90% of the total tree biomass, contained between 15% (plot DC) and 20% (plot RL) of the Si accumulated in the stand. Annual tissues, such as fine roots and litterfall, contained more than approximately half (from 56% in plot RL to 58% in plot DC for fine roots) and a quarter (from 23% in plot RL to 26% in plot DC for litterfall) of the Si contained in the stand. High Si deposition in plant tissues enhances their strength and rigidity but also improves their resistance to plant diseases by stimulating defence reaction mechanisms (Epstein, 1999; Richmond and Sussman, 2003). The

high amount of Si accumulated in beech fine roots resulted not only from a higher Si concentration in this compartment (4.9 to 15.0 g kg^{-1}) but also from an important biomass. The Si content in beech fine roots was very higher (2 to 6 times) than that measured by Maguire et al. (2017) for another deciduous species, i.e. sugar maple (*Acer saccharum*) but in a cooler environment. Besides Maguire et al. (2017) demonstrated in this study that increased soil freezing significantly lowers the Si content of sugar maple fine roots... The beech fine root biomass ranged from 7.3 to 10.6 t.ha^{-1} on the Montiers site. These values correspond to the upper part of the range of 2.4 to 9.6 t.ha^{-1} reported in the literature for beech stands in Europe (Hendrik and Bianchi, 1995; Le Goff and Ottorini 2001; Schmid, 2002, Claus and George 2005; Bolte and Villanueva, 2006) and are in agreement with the fine root biomass determined for another beech forest located in the northeastern France (7.4 to 9.8 t.ha^{-1}; Bakker et al., 2008).

Because most of the Si accumulated in leaves and fine roots with rapid turnover (annual for leaves and estimated at 1.11±0.21 y^{-1} for beech fine roots; Brunner et al., 2013), the main part of the Si taken up by trees returned to the soil each year via litterfall degradation (28%, from 25.2 kg ha^{-1} in plot RL to 44.9 kg ha^{-1} in plot DC) and via the decomposition of fine root necromass (approximately 71%, from 67.9 kg ha^{-1} in plot RL to 109.5 kg ha^{-1} in plot DC) (Figure 6, Table 2). As demonstrated by Sommer et al. 2013, only a small fraction (approximately 1%; from 1.0 kg ha^{-1} in plot RL to 1.8 kg ha^{-1} in plot DC) of the Si taken up by the tree stand accumulated each year in the perennial tree compartments, i.e., the stem, branch and coarse roots (Figure 6, Table 2). As a consequence, approximately 99% of the Si taken up by the stand each year returned to the soil via recycling of fine roots and leaves. The Si amount accumulated in the tree stand and returning to the soil (without considering the exploitation residuals) in the Montiers site ranged from 93 kg ha^{-1} y^{-1} to 154 kg ha^{-1} y^{-1}. The Si accumulated is higher than in other beech ecosystems previously studied, i.e., 20 kg ha^{-1} y^{-1} (Cornelis et al, 2010a) and 34 kg ha^{-1} y^{-1} (Sommer et al. 2013), mainly because the role of fine roots in the Si cycle was underestimated in previous studies. For example, Gérard et al. (2008), who modelled the cycle of Si in the soil of a temperate forest, estimated that the Si amount accumulated in Douglas fir roots was less than 1% of the total uptake.

4.2 Si residence time and budget in the forest floor

Because the amount of Si in the small wood was negligible in the three plots in comparison to the organic horizons (< 3% of the Si contained in the forest floor), only the organic horizons will be discussed below.

4.2.1 Mineral soil content in organic horizons

Cornelis et al. (2010a) estimated that the proportion of soil with a moder humus type was approximately 40% for a deciduous temperate forest. In our study, we determined that the fraction of soil mixed in the organic horizons, i.e., mull form, did not surpass 5%. The higher rate of soil pollution in the study of Cornelis et al. (2010a) can be explained by the presence of a thick Oh layer in the moder that was in direct contact with the superficial soil layer and was characterized by an intense mixing of degraded organic matter with soil particles, induced by biological activities, mainly bioturbation by earthworms in these soils (Lavelle, 1988). The Si input by dust deposits in the organic horizons was negligible, with a maximum value of 6.0 kg ha^{-1} y^{-1} (no stand interception) in comparison with a stock of 151 to 246 kg ha^{-1} of Si in the organic horizons. Lequy et al. (2014), who studied the mineralogy of the dust deposits of the Montiers site, observed that the Si deposits in throughfall was mainly quartz.

4.2.2 Si residence time in organic horizons

The main phytogenic Si input into the organic horizons was opal phytoliths (Krieger et al., 2017), which dissolve slowly (Fraysse et al., 2009) in comparison to the rate of organic matter mineralization. The residence time of Si in the organic horizons is higher than that of carbon (5.3 ± 0.8 vs 1.9 ± 0.4 y). In addition, the presence of testate amoebae, organisms rich in Si (Figure 1; Sommer et al., 2013), in the organic horizons suggests that a part of the Si from the phytoliths belonged to the protozoic Si pool. Sommer et al. (2013) estimated that testate amoebae may use half of the Si input by litterfall in beech organic horizons (17 kg ha^{-1} vs 34 kg ha^{-1}) for shell synthesis.

4.2.3 Si budget in organic horizons

During the study period (2012-2015), the Si input in the organic horizons via litterfall were primarily higher than the Si output via soluble transport (assessed in ZTL solutions under the forest floor) for the three soils. This net flux of Si should have induced the accumulation of Si in the organic horizons, what we did not observe in the four years of the study. This suggests the existence of another output flux which was not quantified in our study. This flux is likely the solid particulate migration toward the topsoil layer, as demonstrated by Ugolini et al. (1977). These authors observed that organic particles containing notably silicon were predominant in the migrant material in the upper soil horizons. In our study, the solid particulate migration from the organic horizons to the topsoil may consist of the colloid transport of amoebae (Harter et al., 2000) or the transport of phytoliths (Fishkis et al. 2010). These latter observed, though a field study using fluorescent labelling, that the downrard transport distance of phytoliths after one year was 3.99± 1.21 cm for a Cambisol with a preferential translocation of small-sized phytoliths..

4.3 Si budget and origin in soil

The Si production (51 6) in the soil mainly results from pedogenic Si from soil mineral dissolution and from biogenic Si from plant tissues and testate amoebae (Cornelis et al., 2011; Sommer et al., 2013; Puppe et al., 2015). The immobilization (sink) of dissolved Si in the soil is due to plant and organism immobilization and precipitation of secondary minerals, such as phyllosilicates or Si-bearing short range organization minerals or allophane, immogolite (Dahlgren and Ugolini, 1989; Ma and Yamaji, 2006; Sommer et al., 2013; Tubana et al., 2016; Kabata-Pendias and Mukherjee, 2007).

A net production of dissolved Si in the soils was observed on the three studied plots down to a depth of 60 cm, showing a positive production/immobilization budget. The net production of Si in the soil, ranging from 7.0 to 16.7 kg ha^{-1} y^{-1}, was mainly located in the 0-10 cm layer, which probably accumulated amorphous Si from organic horizons that contained a large portion of fine roots from the soil. This is corroborated by the strong relationship between annual Si production in the 10-60 cm soil layers and fine root content (data not shown, $r^2 = 0.94$). The contribution of fine roots to the production of dissolved Si was higher in the superficial layer and decreased in the deep soil layers. A peak of net Si production was observed during fall (except in the deeper soil layer; Figure 3), which was probably due to an increase in Si production through the decomposition of dead roots. This finding is consistent with the studies of Meier and Leuschne (2008) and Konopka (2009), who demonstrated that fine root necromass is highest at the end of the summer, when the soil is the driest, favouring root mortality. At our site, this period was also characterized by a maximum concentration of Si in the bound waters and a negative budget

in the 10-cm to 60-cm soil layer, resulting from the precipitation of secondary minerals. As a result, a drastic decrease of Si production was observed in the surface layer during the vegetation period, where Si uptake by plants occurred (Figure 3). In the deeper layer, the dissolved Si budget was significantly negative and likely corresponded to mineral precipitation, induced by a decrease of Si drainage with the depth, as observed by Sommer et al. (2013). The Si produced in the soils was mainly leached out of the soil profile by drainage during winter. The annual drainage flux ranged from 21 to 27 kg Si ha^{-1} y^{-1} in the three soils of the Montiers site which is higher than those measured in other beech forests by Bartoli (1983; 0 kg Si ha^{-1} y^{-1}), Cornelis et al. (2010b, 6 kg Si ha^{-1} y^{-1}), Sommer et al. (2013; 14 kg Si ha^{-1} y^{-1}), and Clymans et al. (2011; 18 kg Si ha^{-1} y^{-1}). The differences can result from multiple factors, i.e., topography, soil properties (texture, structure, pH), rainfall (level and intensity) and other climatic factors, and stand characteristics (tree species and age, stem density, ground vegetal cover…). In our study, the Si leached out of the soil profile was negligible compared to the Si taken up by trees, i.e., ratios of 1:4 to 1:7 in RL and DC, respectively. If we deduce the part of Si leached from the organic horizons, these ratios rise to about 1:5 to 1:22 in RL and DC. Because biogenic Si in general is more soluble than lithogenic or pedogenic Si (Fraysse et al., 2009 ; Cornelis and Delvaux, 2016), very few of the Si leached within the soil profile directly results from the dissolution of soil minerals, as demonstrated in other studies in temperate forests (Bartoli, 1983; Watteau and Villemin, 2001; Gerard et al, 2008; Cornelis et al., 2010a; Cornelis et al., 2011a; Sommer et al., 2006; Sommer et al., 2013).

4.4 Si cycle at stand scale

Silicon inputs and outputs have minor contributions to the Si budget in our forest ecosystem, and the Si cycle is mainly driven by internal fluxes, especially recycling of biogenic Si. However, Struyf et al. (2010) observed that land use is the most important controlling factor of Si mobilization in European watersheds. These authors showed that deforestation and conversion to agricultural land or other land uses leads to a twofold to threefold decrease in baseflow delivery of Si.

As explained above, the main part of the Si taken up by trees was allocated to annual compartments, i.e., 28% to leaves, buds, beechnuts and fruit capsules and 71% to fine roots (Figure 6). Only 1% of the Si taken up by trees was allocated to perennial tissues, i.e., stem and branches, coarse roots (Figure 6). In addition, about half of the Si accumulated in the perennial tree compartments returned each year to the soil via branch falls and exploitation residues (< 7 cm diameter branches left on the floor and small/coarse roots left in the soil) and approximately 40% was exported out of the site (stem and > 7 cm diameter branches). As a result, the amount of Si immobilized in trees remained almost constant over time at the stand scale (mean Si immobilization for the three plots, 0.1 kg ha^{-1} y^{-1}).

In the organic horizons and in the soil, mainly in the 0-10 cm layer, we observed a high net Si production, likely resulting from the decomposition of litter leaves and testate amoebae in the organic horizons and of fine roots in the soil (Figure 6). The seasonal dynamics of net Si production during the year suggest a relationship between biological activities and Si production, i.e., high net Si production at the end of the summer is linked to fine root decomposition and lower net Si production during spring/summer is induced by tree uptake. Net Si production decreased with depth, and a immobilization of Si was observed in the deeper soil horizon in plot DC (Figure 6). This likely resulted from both a decrease in Si production (less root and clay) and the precipitation of Si through the formation of secondary minerals, resulting from reduced drainage flux.

The assessment of Si fluxes and pools in the different compartments of our forested site coupled with a seasonal dynamic follow-up reveal a rapid and almost total recycling of Si in our site and show the strong biological influence, mainly fine roots, and processes in the Si cycle.

4.5 Soil influence in the soil Si inputs/outputs

.

We showed that the Si content of plant compartments (leaves, organic horizons, aboveground and belowground biomasses) were higher in the Si rich soils (plots DC and EC) compared to plot RL. This is in agreement with the observations of Heineman et al. (2016) in tropical forests, which demonstrated that nutrient concentrations in wood and leaves correlated positively with soil Ca, K, Mg and P concentrations in soils. The concentration of dissolved Si in the soil is known to influence opal formation in plants (Cornelis et al., 2010b) but phytolith production seems to be more affected by the phylogenetic position of a plant than by environmental factors (Hodson et al., 2005). For example, these authors demonstrated through meta-analysis of the data, that in general ferns, gymnosperms and angiosperms accumulated less Si in their shoots than non-vascular plant species and horsetails. Moreover, the annual tree compartments (leaves and fine roots) were more concentrated in Si than the perennial compartments (branches, stem and coarse roots). Silicon plays several physiological and ecological functions in leaves and roots, such as an involvement in the detoxification of aluminum, oxalic acid, and heavy metals, in the regulation of ion balance, in the reduction of hydric, salt, and temperature stresses (Currie and Perry, 2007; Meunier et al., 2017). They also contribute to the optimization of photosynthesis by gathering and scattering light in the leaves, confer mechanical support and tissue rigidity, and facilitate pollen release, germination, and tube growth (Bauer, Elbaum, & Weiss, 2011; Currie and Perry, 2007; Gal et al.,, 2012). In addition to these physiological functions, Si has also ecological significance by protecting plants against herbivores and phytopathogens (Currie and Perry, 2007; Lins et al., 2002). The variations of Si content in the annual tree compartments induced by the soil type significantly affected the Si fluxes in the ecosystem. The annual uptake and Si recycling (leaves + buds, beechnuts, fruit capsules + fine roots) were 127.2 and 154.0 kg ha^{-1}, respectively, in plot DC, as opposed to 94.8 and 92.7 kg ha^{-1}, respectively, in plot RL.

In return, the bound solutions were more concentrated in plot RL compared to plot DC. This is partly due to the higher clay content in plot RL compared to plot DC (clay was two times higher in plot RL). This considerably increases the specific surface area of minerals and improves their weatherability and water retention capacity (Carroll and Starkey, 1971; De Jonge et al., 1996).

5 Conclusion

By coupling different approaches (annual budget in solid vegetal and solution phases and monthly dynamics of solutions) and methods (direct *in situ* measurements and standard and site specific modelling) to quantify Si pools and fluxes in the different ecosystem compartments, our study allowed us to assess the Si cycle at the forest stand scale. Interestingly, our study highlights the main contribution of fine roots and, to a lesser extent, of leaves in the Si cycle (Figure 7). Almost all the dissolved Si was taken up by trees at any given time (very weak leaching out of the soil profile) and was recycled each year (approximately 99%, only 1% immobilized in perennial tissues). This suggests that Si cycle is almost closed during the vegetation period; dissolved Si is taken up by vegetation then Si returned to the soil mainly through root and leave decomposition in the form of dissolved Si, which is

again taken up by vegetation. This observation is consistent with the observation of Sommer et al. (2013), who demonstrated a low contribution of geochemical weathering processes to the Si cycle in a forest biogeosystem on a decadal time scale. The seasonal dynamics of dissolved Si confirmed the key role of biological processes in the Si cycle, notably through the production of dissolved Si during the decomposition of fine roots. Our study also revealed that soil type influences the Si accumulation in tree and the Si production in the soil. The plant compartments were Si-enriched in the soil with higher Si concentration, i.e., DC (plot DC) compared to plant compartments in the RL (plot RL), resulting in 1.6-times higher recycling in plot DC compared to plot RL. While Si release was relatively similar in the organic horizons for the three plots, its production in the soil, mainly in the 0-10 cm layer, was twice higher in plot RL and richer in clays than plot DC.

Further research is needed in the mid-term (i) to assess the mineralisation speed of fine roots in the soil and the speed of transformation of the BSi of roots into DSi, (ii) determine the annual and seasonal fate of the Dsi issued from roots, between uptake, mineral precipitation, drainage, fixation by organisms, and (iii) quantify the vertical transfer of solid particulates between organic horizons and topsoil.

Acknowledgement

We acknowledge S. Didier for site implementation and management, L. Franoux and A. Genêt for the development of allometric equations, C. Pantigny, L. Gelhaye, B. Simon, C. Nys, J. Mangin, C. Goldstein, F. César, M. D'Arbaumont and M. Simon for technical help, Salsi, L. for preparing the samples and performing the SEM and EDX analyses, and the ONF officers for the management of the Montiers forest. We would like to thank the National Forest Office (ONF) for welcoming us into the domanial forest of Montiers and for the management of the forest. The authors acknowledge the facilities of the French National Institute for Agricultural Research and the Service d'Analyse des Roches et des Minéraux of the French National Center for Scientific Research. This work was supported by the Andra and INRA (accord spécifique N°9) and GIP-Ecofor (contract N°1138451B). The Montiers site belongs to the SOERE F-ORE-T (http://www.gip-ecofor.org/f-ore-t/index.php), AnaEE France (http://www.anaee-s.fr/) and ICOS (www.icosinfrastructure.eu) networks.

The authors declare that they have no conflict of interest.

References

Alexandre, A., Meunier, J. D., Colin, F., and Koud, J. M.: Plant impact on the biogeochemical cycle of silicon and related weathering processes, Geochim. Cosmochim. Ac., 61, 677–682, 1997.

Alexandre, A., Bouvet, M., and Abbadie, L.: The role of savannas in the terrestrial Si cycle: A case study from Lamto, Ivory Coast, Global Planet. Change, 78, 162–169, 2011.

Bakker, M. R., Turpault, M. P., Huet, S., and Nys, C.: Root distribution of *Fagus sylvatica* in a chronosequence in western France, For. Res. 13, 176-184, 2008.

Bartoli, F. and Souchier, B., Cycle et rôle du silicium d'origine végétale dans les écosystèmes forestiers tempérés, Ann. Sci. For., 35, 187–202, 1978.

Bartoli, F., and Wilding, L. P.: Dissolution of biogenic opal as a function of its physical and chemical properties1, Soil Sci. Soc. Am. J., 44, 873-878, 1980.

Bauer, P., Elbaum, R., and Weiss, I. M.: Calcium and silicon mineralization in land plants: Transport, structure and function. Plant Sci., 180, 746–756, 2011.

Biermans, V. and Baert, L.: Selective extraction of the amorphous Al, Fe and Si oxides using an alkaline Tiron solution, Clay Miner., 12, 127–135, 1977.

Blecker, S. W., McCulley, R. L., Chadwick, O. A., and Kelly, E. F.: Biologic cycling of silica across a grassland bioclimosequence, Global Biogeochem. Cy., 20, 2006.

Bolte, A., and Villanueva, I.: Interspecific competition impacts on the morphology and distribution of fine roots in European beech (*Fagus sylvatica* L.) and Norway spruce (*Picea abies* (L.) Karst.), Eur. J. For. Res., 125, 15–26, 2006.

Brunner, I., Bakker, M. R., Bjork, R. G., Hirano, Y., Lukac, M., Aranda, X., Borja, I., Eldhuset, T. D., Helmisaari, H. S., Jourdan, C., Konopka, B., Miguel Perez, C., Persson, H., and Ostonen, I.: Fine-root turnover rates of European forests revisited: an analysis of data from sequential coring and ingrowth cores Plant Soil, 362 (1-2), 357-372, 2013.

Cai, K., Gao, D., Luo, S., Zeng, R., Yang, J., and Zhu, X.: Physiological and cytological mechanisms of silicon-induced resistance in rice against blast disease, Physiol. Plant 134, 324–333, 2008.

Calvaruso, C., Kirchen, G., Saint-André L., Redon, P.-O., and Turpault, M.-P.: Relationship between soil nutritive resources and the growth and mineral nutrition of a beech (*Fagus sylvatica*) stand along a soil sequence, Catena, 155, 156-169, 2017.

Carey, J. C., Parker, T. C., Fetcher, N., and Tang, J.: Biogenic silica accumulation varies across tussock tundra plant functional type, Funct. Ecol., 31, 2177-2187, 2017.

Carroll, D., and Starkey, H. C.: Reactivity of clay minerals with acids and alkalies, Clay Clay Miner. 19, 321–333, 1971.

Claus, A., and George, E: Effect of stand age and fine-root biomass and biomass distribution in three European forest chronosequences, Can. J. For. Res., 35, 1617-1625, 2005.Clymans W., Struyf E., Govers G., Vandevenne F., Conley D. J.: Anthropogenic impact on biogenic Si pools in temperate soils, Biogeosciences, 8, 2281–2293, 2011.

Cornelis, J. T., Ranger, J., Iserentant, A., and Delvaux, B.: Tree species impact the terrestrial cycle of silicon through various uptakes, Biogeochemistry, 97, 231–245, 2010a.

Cornelis, J. T., Delvaux, B., Cardinal, D., Andre, L., Ranger, J., and Opfergelt, S.: Tracing mechanisms controlling the release of dissolved silicon in forest soil solutions using Si isotopes and Ge/Si ratios, Geochim. Cosmochim. Ac., 74, 3913–3924, 2010b.

Cornelis, J. T., Titeux, H., Ranger, J., and Delvaux, B.: Identification and distribution of the readily soluble silicon pool in a temperate forest below three distinct tree species, Plant Soil, 342, 369–378, 2011.

Cornelis, J. T., and Delvaux, B.: Soil processes drive the biological silicon feedback loop, Funct. Ecol., 30, 1298–1310, 2016.

Currie, H. A., and Perry, C. C.: Silica in plants: Biological, biochemical and chemical studies. Ann. Bot., 100, 1383–1389, 2007.

De Jonge, L. W., Moldrup, P., Jacobsen, and O. H., Rolston, D. E.: Relations between specific surface area and soil physical and chemical properties, Soil Sci., 161(1), 9-21, 1996.

Dixon, J. B., and Weed, S. B.: Minerals in soil environments, Second Edition. SSSAJ, Madison, 1989.

Drees, L. R., Wilding, L. P., Smeck, N. E., and Senkayi, A. L.: Silica in soils: quartz and disorders polymorphs. In: Dixon JB, Weed SB (eds) Minerals in soil environments. Soil Science Society of America, Madison, pp. 914–974, 1989.

Emsens, W. J., Schoelynck, J., Grootjans, A. P., Struyf, E., Van Diggelen, R. : Eutrophication alters Si cycling and litter decomposition in wetlands, Biogeochemistry, 130, 289-299, 2016.

Epstein, E. Silicon, Annu. Rev. Plant Physiol, Plant Mol. Biol., 50, 641–664, 1999.

FAO, 2016. World reference base for soil resources 2014. In: World Soil Resources Report 106. FAO, Rome.

Finér, L., Ohashib, M., Noguchic, K., Hiranod, Y.: Factors causing variation in fine root biomass in forest ecosystems, For. Ecol. Manga., 261, 265-277, 2011.

Fishkis, O., Ingwersen, J., Lamers, M., Denysenko, D., and Streck T.: Phytolith transport in soil: A field study using fluorescent labelling, Geoderme, 157, 27-36, 2010.

Fraysse, F., Pokrovsky, O. S., Schott, J., and Meunier, J. D.: Surface chemistry and reactivity of plant phytoliths in aqueous solutions, Chem. Geol., 258, 197–206, 2009.

Gal, A., Brumfeld, V., Weiner, S., Addadi, L., and Oron, D.: Certain biominerals in leaves function as light scatterers. Adv. Mater., 24, 77–83, 2012.

Gaul, D., Hertel, D., Leuschner, C.: Estimating fine root longevity in a temperate Norway spruce forest using three independent methods, Funct. Plant Biol., 36, 11–19, 2009.

Gérard, F., Mayer, K. U., Hodson, M. J., and Ranger, J.: Modelling the biogeochemical cycle of silicon in soils: application to a temperate forest ecosystem, Geochim. Cosmochim. Acta 72(3), 741–758, 2008.

Gordon, W. S., and Jackson, R. J.: Nutrient concentrations in fine roots, Ecology, 81, 275-280, 2000.

Granier, A., Bréda, N., Biron, P., Villette, S.: A lumped water balance model to evaluate duration and intensity of drought constraints in forest stands, Ecol. Model. 116, 269–283, 1999.

Harter, T., Wagner, S., and Atwill, E. R.:Colloid transport and filtration of Cryptosporidium parvum in sandy soils and aquifer sediments, Environ. Sci. Technol., 34, 62-70, 2000.He, C. W., Ma, J., and Wang, L. J.: A hemicellulose-bound form of silicon with potential to improve the mechanical properties and regeneration of the cell wall of rice, New Phytol. 206, 1051–1062, 2015.

Heineman, K. D., Turner, B. L., and Dalling, J. W.: Variation in wood nutrients along a tropical soil fertility gradient, New pytol., 211, 440-454, 2016.

Hendriks, C. M. A., and Bianchi, F. J. J.A.: Root density and root biomass in pure and mixed forest stands of Douglas-fir and Beech. Neth. J. Agric. Sci., 43, 321-331, 1995.

Henry, M., Picard, N., Trotta, C., Manlay, R., Valentini, R., Bernoux, M., Saint-André, L.: Estimating tree biomass of sub-Saharan African forests: a review of available allometric equations, Silva Fenn., 45, 477–569, 2011.

Iler, R. K.: The chemistry of silica, Wiley-Interscience, New York, 1979.

Hodson, M. J., White, P. J., Mead, A., and Broadley, M. R.: Phylogenetic variation in the silicon composition of plants. Ann. Bot., 96, 1027-1046, 2005.

Jones, L. H. P., and Handreck, K.A.: Studies of silica in the oat plant. III. Uptake of silica from soils by plant, Plant Soil, 23(1), 79–96, 1965.

Jourdan, C., Silva, E. V., Goncalves, J. L. M., Ranger, J., Moreira, R. M., and Laclau, J. P.: Fine root production and turnover in Brazilian Eucalyptus plantations under contrasting nitrogen fertilization regimes, For. Ecol. Manage., 256, 396-404, 2008.

Kabata-Pendias, A., and Mukherjee, A. B.: Trace elements from soil to Human, Springer, Berlin, 2007.

Kelly, E. F., Chadwick, O. A., Hilinski, T. E.: The effect of plants on mineral weathering, Biogeochemistry 42, 21–53, 1998.

Kirchen, G., Calvaruso, C., Granier, A., Redon, P.-O., Van Der Heijden, G., Bréda, N., and Turpault, M.-P. Effect of soil type and precipitation level on the water budget of a beech forest: Consequence on stand growth, For. Ecol. Manage., 390, 89-103, 2017.

Kodama, H. and Ross, G. J.: Tiron dissolution method used to remove and characterize inorganic components in soils, Soil Sci. Soc. Am. J., 55, 1180–1187, 1991.

Konôpka, B.: Differences in fine root traits between Norway spruce (*Picea abies* (L.) Karst.) and European beech (*Fagus sylvatica* L.)—a case study in the Kysucké Beskydy Mts, J. For. Sci., 55, 556–566, 2009.

Krieger, C., Calvaruso, C., Morlot, C., Uroz S., Salsi, l., and Turpault M.-P.: Identification, distribution, and quantification of biominerals in a deciduous forest, Geobiology, 15, 296-310, 2017.

Lavelle, P.: Earthworm activities and the soil system, Biol. Fert. Soils, 6, 237-251, 1988.

Le Goff, N., and Ottorini J.-M.: Root biomass and biomass increment in a beech (*Fagus sylvatica L.*) stand in North-East France, Ann. For. Sci., 58 (1),1-13, 2001.

Legout, A., Legout, C., Nys, C., Dambrine, E.: Preferential flow and slow convective chloride transport through the soil of a forested landscape (Fougères, France), Geoderma 151, 179-190, 2009.

Lequy, E., Calvaruso, C., Conil, S., Turpault, M.-P.: Atmospheric particulate deposition in temperate deciduous forest ecosystems: Interactions with the canopy and nutrient inputs in two beech stands of Northeastern France, STOTEN, 487, 206-215, 2014.

Lins, U., Barros, C. F., da Cunha, M., and Miguens, F. C.: Structure,morphology, and composition of silicon biocomposites in the palm tree *Syagrus coronata* (Mart.), Becc. Protoplasma, 220, 89–96, 2002.

Lucas, Y., Luizao, F. J., Chauvel, A., Rouiller, J., and Nahon, D.: The relation between biological activity of the rain forest and mineral composition of soils, Science, 260, 521–523, 1993.

Ma, J. F., and Yamaji, N.: Silicon uptake and accumulation in higher plants. Trends Plant Sci., 11(8), 392–397, 2006.

Maguire, T. J., Templer, P. H., Battles, J. J., and Fulweiler, R. W.: Winter climate change and fine root biogenic silica in sugar maple trees (*Acer saccharum*): Implications for silica in the Anthropocene. J. Geophys. Res. Biogeosci., 122, 708-715, 2017.

Massey, F. P., and Hartley, S. E.: Physical defences wear you down: progressive and irreversible impacts of silica on insect herbivore, J. Anim. Ecol., 78, 281-291, 2009.

Mc Keague, J. A. and Cline, M. G.: Silica in soil solutions I. The form and concentration of dissolved silica in aqueous extracts of some soils, Can. J. Soil Sci., 43, 70–82, 1963.

Meunier, J. D., Barboni, D., Anwar-ul-Haq, M., Levard, C., Chaurand, P., Vidal, V., Grauby, O., Huc, R., Laffont-Schwob, I., Rabier, J., and Keller, C.: Effect of phytoliths for mitigating water stress in durum wheat, New Phytol., 215, 229–239, 2017.

Meier, I. C., and Leuschner, C.: The belowground drought response of European beech: fine root biomass and carbon partitioning in 14 mature stands across a precipitation gradient, Glob. Change Biol., 14, 2081–2095, 2008.

Mitani, N., and Ma, J. F.: Uptake system of silicon in different plant species, J. Exp. Bot., 56, 1255–1261, 2005.

Piperno, D. R.: Phytolith analysis: an archaeological and geological perspective, Academic Press, San Diego, 1984.

Puppe, D., Ehrmann, O., Kaczorek, D., Wanner, M., and Sommer, M.: The protozoic Si pool in temperate forest ecosystems âA˘T Quantification, abiotic controls ˘ and interactions with earthworms. Geoderma, 243, 196-204, 2015.

Puppe, D., Höhn, A., Kaczorek, D., Wanner, M., Wehrhan, M., and Sommer, M.: How big is the influence of biogenic silicon pools on short-term changes in water-soluble silicon in soils? Implications from a study of a 10-year-old soil–plant system. Biogeosciences, 14, 5239-5252, 2017

Richmond, K. E., and Sussman, M.: Got silicon? The non-essential beneficial plant nutrient, Curr. Opin. Plant Biol., 6, 268–272, 2003.

Saccone, L., Conley, D. J., Koning, E., Sauer, D., Sommer, M., Kaczorek, D., Blecker, S. W. and Kelly, E. F.: Assessing the extraction and quantification of amorphous silica in soils of forest and grassland ecosystems, Eur. J. Soil Sci., 58, 1446–1459 2007.

Saint-André, L., M'Bou, A. T., Mabiala, A., Mouvondy, W., Jourdan, C., Rouspard, O., Deleporte, P., Hamel, O., and Nouvellon, Y.: Age related equation for above and below ground biomass of a Eucalyptus in Congo. For. Ecol. Manage., 205, 199–214, 2005.

Schmid, I.: The influence of soil type and interspecific competition on the fine root system of Norway spruce and European beech, Basic Appl. Ecol. 3, 339–346, 2002.

Sommer, M., Kaczorek, D., Kuzyakov, Y., and Breuer, J.: Silicon pools and fluxes in soils and landscapes – a review, J. Plant Nutr. Soil Sci., 169, 310–329, 2006.

Sommer, M., Jochheim, H., Höhn, A., Breuer, J., Zagorski, Z., Busse, J., Barkusky, D., Meier, K., Puppe, D., Wanner, M., and Kaczorek, D.: Si cycling in a forest biogeosystem – the importance of transient state biogenic Si pools, Biogeosciences, 10, 4991-5007, 2013.

Struyf, E., Van Damme, S., Gribsholt, B., Bal, K., Beauchard, O., Middelburg, J. J., Meire, P: Phragmites australis and silica cycling in tidal wetlands, Aquat. Bot., 87, 134-140, 2007.

Struyf, E., Smis, A., Van Damme, S., Garnier, J., Govers, G., Van Wesemael, B., Conley, D., Batelaan, O, Clymans, W., Vandevenne, F., Lancelot, C., Goos, P., and Meire, P.: Historical land use change has lowered terrestrial silica mobilization. Nature comm, 1, 129-135, 2010.Takahashi, E., Ma, J. F., and Miyake, Y.: The possibility of silicon as an essential element for higher plants, Comment. Agric. Food Chem., 2, 99–102, 1990.

Tubana, B. S., Babu, T., and Datnoff, L. E.: A review of silicon in soils and plants and its role in us agriculture: history and future perspectives, Soil Sci., 181, 393-411, 2016.

Ugolini, F. C., Dawson, H., and Zachara, J.: Direct evidence of particle migration in the soil solution of a podzol, Science, 4317, 603-605, 1977.

White, A. F., Vivit, D. V., Schulz, M. S., Bullen, T. D., Evett, R. R., and Aagarwal, J. : Biogenic and pedogenic controls on Si distributions and cycling in grasslands of the Santa Cruz soil chronosequence, California, Geochim. Cosmochim. Ac., 94, 72–94, 2012.

Yuan, Z. H., and Chen, H. Y. H.: Fine root biomass, production, turnover rates, and nutrient contents in boreal forest ecosystems in relation to species, climate, fertility, and stand age: Literature review and meta-analyses, Crit. Rev. Plant Sci., 29, 204-221, 2010.

Figure caption

Fig. 1: Si in biological tissues of beech trees observed through Scanning Electron Microscopy. (a) Si precipitates in the intercellular space of fresh leaves, forming phytoliths (vertical white arrow). Deposits of Si (white arrows) in the inner cell walls of fruit capsules (b), stem bark (dand e), bud scales (f), and roots (g, h, and i). (c) Hyphae, testate amoebae and large voids in aged litter leaves. Si deposits only present in the testate amoeba shells (horizontal empty white arrows). The presence of Si was confirmed with EDX (analyzed zones indicated by white vertical arrows).

Fig. 2: Seasonal dynamics on four years (January 2012 to December 2015) of dissolved Si concentration in throughfall solution for the three plots DC, EC, and RL.

Fig. 3: Seasonal dynamics over four years (January 2012 to December 2015) of the dissolved Si budget in the different layers (forest floor: FF; soil 0-10 cm: L0-10; soil 10-30 cm: L10-30; soil 30-60 cm: L30-60; and soil 60-90 cm: L60-90) for the three plots DC, EC, and RL.

Fig. 4: a. Mean dissolved Si concentration over four years (January 2012 to December 2015) in a zero-tension lysimeter (ZTL) and tension lysimeter (TL) with soil solutions at different depths (0-10 cm, 10-30, 30-60, and 60-90 cm) in plots DC and RL. B. Seasonal dynamics over four years (January 2012 to December 2015) of Si concentrations in ZTL and TL soil (TL) in the layers 0-10 cm (L0-10) and 10-30 cm (L10-30) of plot RL.

Fig. 5: Mean annual dissolved Si budget in the different layers of the forest floor, FF; soil 0-10 cm: L0-10; soil 10-30 cm: L10-30; soil 30-60 cm: L30-60; and soil 60-90 cm: L60-90) for the three plots DC, EC, and RL. Bars represent the standard deviations. Positive and negative values represent the production or immobilization of dissolved Si in the given layer. Bars with an asterisk are significantly different from 0, according to a Kruskal-Wallis test at the threshold P value level of 0.05.

Fig. 6: Summary scheme of Si cycling on the plots DC, EC and RL of our study forest site, including (i) pools of Si in the biomass, (ii) internal fluxes, i.e., in the soil-plant system, (iii) external fluxes entering or leaving the soil-plant system, and (iv) the dissolved Si budget in the different layers of the ecosystem. Pools are presented by rectangular boxes (tree annual and perennial parts, organic horizons and small dead wood, and soil). Internal fluxes (solid form from the tree to the soil, i.e., fine roots, litterfall including leaves, buds and branches, and exploitation residues; and in solution from the soil to the plant, i.e., the tree uptake) are presented in boxes with rounded edges. Grey/black arrows indicate the direction and the intensity of the internal fluxes. The external fluxes (inputs: rainfall and dust deposits, and outputs: drainage and biomass harvest) are presented in flag boxes. For each pool and flux, values presented are those of the plots DC (in green), EC (in orange), and RL (in blue), respectively. The dissolved Si budget in the different layers (forest floor and different soil horizons) are represented with white arrows, which indicate the direction and the intensity of the fluxes. Arrows leaving the layer indicate the production of dissolved Si in this layer. In contrast, arrows entering the layer indicate the immobilization of dissolved Si in this layer. Values presented in each box and arrow are annual mean values for plots DC, EC, and RL, respectively (except for atmosphere values which are similar for the three plots). The AG and BG correspond to aboveground and belowground tree compartments.

Fig. 7: Summary scheme of the main findings of this study (TS) and comparison with other studies (L).

Table 1: Physicochemical properties of the three studied soils in the Montiers site (plot DC; plot EC; plot RL). Presented are the mean values for bulk density (g cm^{-3}), textural distribution (g kg^{-1}), total rock volume (RV), soil water holding capacity (SWHC), soil water pH, organic matter content (OM), cation exchange capacity (CEC; cmol+ kg^{-1}) and base-cation saturation ratio (S/CEC, with S = sum of base cations). Standard deviation values are given in italic. Table adapted from Kirchen et al. (2017).

	Depth	B. density	Clay	F. silt	C. silt	F. sand	C. sand	RV	SWHC	pH_{water}	OM	CEC	S/CEC
	cm	g cm^{-3}	g kg^{-1}					%	mm		g kg^{-1}	cmol + kg^{-1}	%
S1 Dystric Cambisol	0–5	0.98	255	281	160	185	121	1.4	8.2	4.9	68	6.7	64
		0.12	*25*	*24*	*17*	*36*	*19*				*22*	*3.0*	*23*
	5–15	0.94	245	276	162	184	131	1.4	16.5	4.8	43	4.2	35
		0.17	*26*	*29*	*17*	*40*	*24*				*16*	*2.2*	*21*
	15–30	1.23	268	280	161	170	115	1.8	22.7	4.8	26	3.5	26
		0.22	*28*	*31*	*21*	*44*	*31*				*9*	*0.9*	*14*
	30–45	1.36	306	262	150	161	119	2.3	22.6	4.9	15	4.3	36
		0.18	*65*	*45*	*27*	*47*	*32*				*5*	*1.6*	*16*
	45–60	1.45	355	229	126	166	141	3.6	18.1	5.1	10	5.7	55
		0.15	*100*	*45*	*31*	*49*	*39*				*2*	*2.6*	*22*
S2 Eutric Cambisol	0–5	1.03	242	242	143	290	83	2.3	9.2	5.4	73	10.1	83
		0.11	*52*	*16*	*13*	*36*	*24*				*26*	*5.4*	*14*
	5–15	0.93	241	246	145	287	82	3.1	18.2	5.2	45	7.8	59
		0.13	*65*	*17*	*13*	*45*	*24*				*29*	*7.3*	*24*
	15–30	1.23	294	234	136	273	64	7.6	19.1	5.3	27	7.7	61
		0.19	*83*	*23*	*17*	*55*	*11*				*13*	*3.9*	*23*
	30–45	1.35	420	188	107	214	71	29.0	14.7	5.3	17	13.2	68
		0.18	*141*	*43*	*31*	*63*	*20*				*8*	*6.9*	*27*
	45–60	1.32	523	154	85	176	63	40.3	10.3	5.4	11	17.8	76
		0.23	*136*	*42*	*32*	*57*	*31*				*4*	*8.8*	*17*
S3 Rendzic Leptosol	0–5	0.88	449	227	123	119	41	2.3	9.8	5.7	109	24.9	98
		0.14	*80*	*54*	*26*	*39*	*15*				*27*	*8.3*	*5*
	5–15	0.98	430	224	114	123	59	4.9	19.2	5.7	71	20.0	94
		0.12	*82*	*56*	*36*	*37*	*21*				*23*	*7.9*	*7*
	15–30	1.06	516	169	77	102	63	36.4	12.5	6.0	42	23.2	99
		0.22	*81*	*50*	*38*	*42*	*24*				*10*	*6.4*	*5*

Table 2: Mean Si contents, pools and fluxes in the biomass of the three soils of the Montiers site. Standard deviation values are given in brackets. Values with different letters are significantly different according to a Kruskal-Wallis test at the threshold P value level of 0.05 (soil effect, DC vs. EC vs. RL).

Plot	Compartment	Biomass pools (t DM ha^{-1})	Biomass increment (t DM ha^{-1} yr^{-1})	Si content (g kg^{-1})	Si pools (kg ha^{-1})	Si fluxes (kg ha^{-1} yr^{-1})
Dystric Cambisol	Leaves	3.8 (0.4) ^{a}	3.8 (0.4) ^{a}	11.3 (1.8) ^{b}	42.7 (4.3) ^{b}	42.7 (4.3) ^{b}
	Branches/twigs with bark	0.3 (0.2) ^{a}	0.3 (0.2) ^{a}	1.1 (0.3) ^{a}	0.3 (0.2) ^{a}	0.3 (0.2) ^{a}
	Buds, beechnuts, fruit capsules	1.1 (1.1) ^{a}	1.1 (1.1) ^{a}	2.4 (1.0) ^{a}	1.8 (0.9) ^{a}	1.8 (0.9) ^{a}
	Total litterfall	5.2 (1.1) ^{a}	5.2 (1.1) ^{a}		44.8 (5.1) ^{b}	44.8 (5.1) ^{b}
	Organic horizons	11.5 (2.0) ^{a}		21.4 (1.6) ^{a}	246.4 (53.1) ^{a}	
	Small wood	7.5 (1.9) ^{a}		0.8 (0.3) ^{a}	6.5 (3.5) ^{a}	
	Forest floor	19.0 (2.7) ^{a}			252.9 (53.1) ^{a}	
	Stem bark	5.5 (0.7) ^{a}	0.5 (0.0) ^{b}	1.70 (0.33) ^{a}	9.4 (1.2) ^{a}	0.65 (0.03) ^{b}
	Stem wood	84.8 (11.7) ^{ab}	6.4 (0.3) ^{b}	0.05 (0.00) ^{a}	4.0 (0.5) ^{a}	0.30 (0.02) ^{a}
	Small branches (B+W)	18.7 (2.5) ^{ab}	1.2 (0.1) ^{b}	0.40 (0.05) ^{a}	7.4 (1.0) ^{a}	0.49 (0.03) ^{b}
	Medium branches (B+W)	10.2 (1.8) ^{ab}	1.1 (0.1) ^{b}	0.26 (0.04) ^{a}	2.6 (0.5) ^{ab}	0.29 (0.02) ^{b}
	Coarse branches (B+W)	5.1 (1.1) ^{ab}	0.8 (0.1) ^{ab}	0.13 (0.04) ^{a}	0.7 (0.1) ^{ab}	0.10 (0.01) ^{b}
	Aboveground biomass	125.8 (17.9) ^{ab}	10.0 (0.5) ^{b}		24.1 (3.3) ^{ab}	1.82 (0.10) ^{b}
	Fine roots (0-10 cm)	3.2 (0.8) ^{a}	3.5 (0.9) ^{a}	12.8 (2.3) ^{b}	39.5 (7.5) ^{a}	43.9 (8.3) ^{a}
	Fine roots (10-30 cm)	2.9 (1.1) ^{a}	3.2 (1.2) ^{a}	15.0 (2.3) ^{c}	43.9 (6.6) ^{b}	48.8 (7.3) ^{b}
	Fine roots (30-60 cm)	0.9 (0.6) ^{a}	1.0 (0.7) ^{a}	12.3	10.5	11.7
	Fine roots (60-90 cm)	0.4 (0.1) ^{a}	0.4 (0.1) ^{a}	12.7	4.7	5.2
	Total fine roots (0-90 cm)	7.3 (1.8) ^{a}	8.0 (2.0)		98.7 (13.5) ^{b}	109.5 (15.0) ^{b}
	Total coarse roots	24.4 (3.5) ^{a}	2.83 (0.47) ^{a}	0.11 (0.15) ^{a}	2.66 (0.39) ^{b}	0.31 (0.05) ^{b}
	Exploitation residues AG		1.3	0.33		0.42
	Exploitation residues BG		1.1	0.11 (0.15) ^{a}		0.12
	Total exploitation residues		2.4			0.54
	Harvests		4.4	0.16		0.71
Eutric Cambisol	Leaves	4.1 (0.5) ^{a}	4.1 (0.5) ^{a}	8.9 (1.6) ^{ab}	35.4 (2.8) ^{ab}	35.4 (2.8) ^{ab}
	Branches/twigs with bark	0.6 (0.4) ^{a}	0.6 (0.4) ^{a}	0.9 (0.2) ^{a}	0.4 (0.2) ^{a}	0.4 (0.2) ^{a}
	Buds, beechnuts, fruit capsules	1.3 (1.1) ^{a}	1.3 (1.1) ^{a}	3.4 (1.9) ^{a}	3.0 (0.5) ^{b}	3.0 (0.5) ^{b}
	Total litterfall	6.0 (1.1) ^{a}	6.0 (1.1) ^{a}		38.7 (3.1) ^{ab}	38.7 (3.1) ^{ab}
	Organic horizons	9.6 (1.4) ^{a}		17.6 (0.8) ^{a}	174.2 (32.8) ^{ab}	
	Small wood	2.6 (1.2) ^{a}		1.8 (1.1) ^{a}	3.9 (1.3) ^{a}	
	Forest floor	12.5 (0.6) ^{a}			178.1 (32.6) ^{ab}	
	Stem bark	6.1 (0.2) ^{a}	0.4 (0.0) ^{ab}	1.53 (0.28) ^{a}	9.3 (0.3) ^{a}	0.39 (0.04) ^{a}
	Stem wood	109.9 (3.8) ^{b}	5.0 (0.6) ^{ab}	0.05 (0.00) ^{a}	5.1 (0.2) ^{a}	0.23 (0.02) ^{a}
	Small branches (B+W)	20.8 (0.7) ^{b}	0.8 (0.1) ^{ab}	0.38 (0.08) ^{a}	7.9 (0.3) ^{a}	0.31 (0.04) ^{ab}
	Medium branches (B+W)	15.2 (0.6) ^{b}	1.0 (0.1) ^{ab}	0.23 (0.05) ^{a}	3.5 (0.1) ^{b}	0.23 (0.02) ^{ab}
	Coarse branches (B+W)	9.8 (0.6) ^{b}	0.9 (0.1) ^{b}	0.10 (0.03) ^{a}	1.0 (0.1) ^{b}	0.09 (0.01) ^{ab}
	Aboveground biomass	164.2 (5.7) ^{b}	8.0 (0.9) ^{ab}		26.9 (0.9) ^{b}	1.25 (0.13) ^{ab}
	Fine roots (0-10 cm)	4.6 (2.1) ^{a}	5.1 (2.4) ^{a}	9.6 (2.9) ^{ab}	44.5 (13.9) ^{a}	49.4 (15.4) ^{a}
	Fine roots (10-30 cm)	4.5 (1.8) ^{a}	5.0 (1.9) ^{a}	8.2 (1.6) ^{b}	37.0 (7.1) ^{b}	41.1 (7.8) ^{b}
	Fine roots (30-60 cm)	1.2 (0.7) ^{a}	1.3 (0.8) ^{a}	7.5	8.7	9.7
	Fine roots (60-90 cm)	0.4 (0.1) ^{a}	0.5 (0.1) ^{a}	-	-	-
	Total fine roots (0-90 cm)	10.6 (4.1) ^{a}	11.7 (4.5)		90.2 (20.8) ^{b}	100.1 (23.1) ^{b}
	Total coarse roots	32.3 (1.2) ^{b}	4.08 (0.16) ^{b}	0.05 (0.08) ^{a}	1.51 (0.05) ^{a}	0.19 (0.01) ^{a}
	Exploitation residues AG		1.4	0.31		0.43
	Exploitation residues BG		1.4	0.05 (0.08) ^{a}		0.06
	Total exploitation residues		2.8			0.50
	Harvests		4.9	0.15		0.72
: Rendzic Leptosol	Leaves	4.0 (0.4) ^{a}	4.0 (0.4) ^{a}	5.6 (1.3) ^{a}	22.2 (3.1) ^{a}	22.2 (3.1) ^{a}
	Branches/twigs with bark	0.5 (0.3) ^{a}	0.5 (0.3) ^{a}	0.7 (0.1) ^{a}	0.3 (0.2) ^{a}	0.3 (0.2) ^{a}
	Buds, beechnuts, fruit capsules	1.2 (0.9) ^{a}	1.2 (0.9) ^{a}	3.2 (1.6) ^{a}	2.6 (0.5) ^{ab}	2.6 (0.5) ^{ab}
	Total litterfall	5.7 (1.0) ^{a}	5.7 (1.0) ^{a}		25.2 (3.4) ^{a}	25.2 (3.4) ^{a}
	Organic horizons	8.8 (1.5) ^{a}		16.9 (1.4) ^{a}	151.3 (22.6) ^{b}	
	Small wood	1.9 (2.4) ^{a}		1.3 (0.7) ^{a}	4.4 (5.7) ^{a}	
	Forest floor	10.9 (2.8) ^{a}			154.3 (25.3) ^{a}	
	Stem bark	6.8 (0.6) ^{a}	0.3 (0.0) ^{a}	1.34 (0.27) ^{a}	9.1 (0.8) ^{a}	0.41 (0.05) ^{ab}
	Stem wood	80.1 (8.3) ^{a}	3.9 (0.5) ^{a}	0.06 (0.03) ^{a}	5.0 (0.5) ^{a}	0.24 (0.03) ^{a}
	Small branches (B+W)	15.0 (1.4) ^{a}	0.6 (0.1) ^{a}	0.29 (0.04) ^{a}	4.3 (0.4) ^{a}	0.18 (0.02) ^{a}
	Medium branches (B+W)	8.6 (1.4) ^{a}	0.6 (0.1) ^{a}	0.19 (0.04) ^{a}	1.6 (0.3) ^{a}	0.11 (0.02) ^{a}
	Coarse branches (B+W)	4.6 (1.0) ^{a}	0.4 (0.1) ^{a}	0.10 (0.03) ^{a}	0.5 (0.1) ^{a}	0.04 (0.01) ^{a}

	Aboveground biomass	115.2 (12.8) [a]	5.8 (0.8) [a]		20.5 (2.1) [a]	0.98 (0.13) [a]
	Fine roots (0-10 cm)	5.1 (1.4) [a]	5.6 (1.6) [a]	7.8 (2.2) [a]	43.5 (14.1) [a]	48.3 (15.6) [a]
	Fine roots (10-30 cm)	3.6 (1.6) [a]	4.0 (1.8) [a]	4.9 (0.8) [a]	17.6 (3.0) [a]	19.6 (3.3) [a]
	Fine roots (30-60 cm)	NS	NS	-	-	-
	Fine roots (60-90 cm)	NS	NS	-	-	-
	Total fine roots (0-30 cm)	8.7 (3.0) [a]	9.6 (3.3)		61.2 (16.0) [a]	67.9 (17.7) [a]
	Total coarse roots	26.0 (3.0) [a]	3.09 (0.44) [a]	0.06 (0.05) [a]	1.62 (0.19) [a]	0.19 (0.03) [a]
	Exploitation residues AG		1.1	0.24		0.27
	Exploitation residues BG		1.0	0.06 (0.05) [a]		0.06
	Total exploitation residues		2.1			0.33
	Harvests		3.9	0.15		0.57

Table 3: Mean total Si content and pool in the fine earth fraction of the three soils of the Montiers site at different depths. Standard deviation values are given in brackets. Values with different letters are significantly different according to a Kruskal-Wallis test at the threshold P value level of 0.05 (soil effect).

Soil type	Compartment	Total Si content ($g\ kg^{-1}$)	Total Si pool ($t\ ha^{-1}$)
Dystric Cambisol	0-10 cm	305 (13) [a]	297 (33) [b]
	10-30 cm	313 (9) [a]	708 (50) [b]
	30-60 cm	296 (18) [b]	1 301 (422) [b]
	60-90 cm	230 (28) [b]	858 (80) [c]
	Total 0-90 cm		3 164 (487) [b]
Eutric Cambisol	0-10 cm	361 (11) [b]	411 (30) [c]
	10-30 cm	360 (13) [b]	791 (127) [b]
	30-60 cm	295 (62) [b]	871 (290) [b]
	60-90 cm	224 (28) [b]	348 (117) [b]
	Total 0-90 cm		2 421 (410) [b]
Rendzic Leptosol	0-10 cm	287 (27) [a]	233 (18) [a]
	10-30 cm	276 (23) [a]	427 (27) [a]
	30-60 cm	175 (37) [a]	42 (27) [a]
	60-90 cm	144 (39) [a]	27 (8) [a]
	Total 0-90 cm		720 (38) [a]

Table 4: Si content and fluxes in the ZTL (Zero Tension Lysimeters) and TL (Tension Lysimeters) solutions of the three soils of the Montiers site. Standard deviation values are given in brackets. Values with different letters are significantly different according to a Kruskal-Wallis test at the threshold P value level of 0.05 (soil effect).

Plot	Level	Si_{ZTL} concentration (mg l^{-1})	Si_{TL} concentration (mg l^{-1})	Si fluxes (kg ha^{-1} y^{-1})
Dystric Cambisol	Rainfall	0.04 (0.08)		0.2 (0.1)
	Throughfall	0.15 (0.18) [a]		1.2 (0.6) [a]
	Stemflow	0.38 (0.32) [a]		0.1 (0.5) [a]
	Stand deposition			1.3 (0.3) [a]
	Forest floor	1.7 (0.8) [a]		13.7 (2.7) [a]
	L-10 cm	2.0 (0.7) [a]	2.9 (1.0) [a]	19.0 (5.6) [a]
	L-30 cm	2.6 (0.4) [a]	3.5 (1.1) [a]	21.4 (8.3) [a]
	L-60 cm	2.6 (0.5) [a]	4.1 (1.4) [a]	22.4 (9.8) [a]
	L-90 cm	2.5 (0.3)	3.7 (0.6)	20.7 (7.4)
Eutric Cambisol	Rainfall	0.04 (0.08)		0.2 (0.1)
	Throughfall	0.16 (0.16) [a]		1.2 (0.6) [a]
	Stemflow	0.53 (0.38) [a]		0.2 (0.6) [a]
	Stand deposition			1.4 (0.6) [a]
	Forest floor	1.5 (0.6) [a]		12.6 (4.2) [a]
	L-10 cm	2.1 (0.7) [a]	3.2 (1.1) [a]	21.6 (4.8) [a]
	L-30 cm	3.5 (1.6) [a]	4.0 (1.1) [a]	25.5 (5.9) [a]
	L-60 cm	2.8 (0.6) [a]	4.5 (1.1) [a]	26.2 (6.6) [a]
Rendzic Leptosol	Rainfall	0.04 (0.08)		0.2 (0.1)
	Throughfall	0.13 (0.14) [a]		1.0 (0.5) [a]
	Stemflow	0.42 (0.41) [a]		0.1 (0.4) [a]
	Stand deposition			1.2 (0.5) [a]
	Forest floor	1.4 (0.8) [a]		10.7 (1.4) [a]
	L-10 cm	2.1 (1.1) [a]	3.8 (1.2) [a]	25.2 (9.9) [a]
	L-30 cm	2.3 (1.0) [a]	4.2 (1.2) [a]	27.4 (9.0) [a]

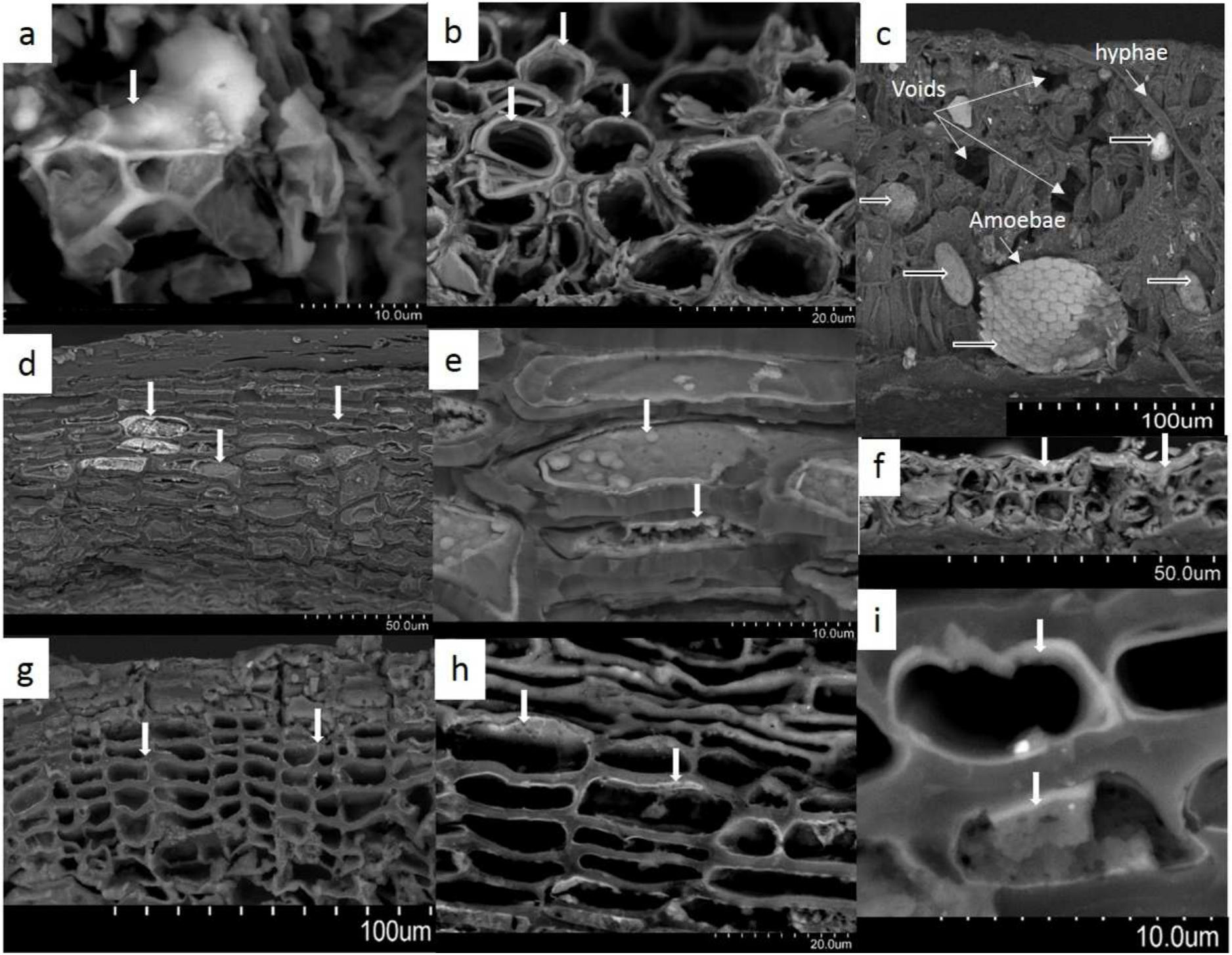
a
10.0um
b
20.0um
c
hyphae
Voids
Amoebae
100um
d
50.0um
e
10.0um
f
50.0um
g
100um
h
20.0um
i
10.0um

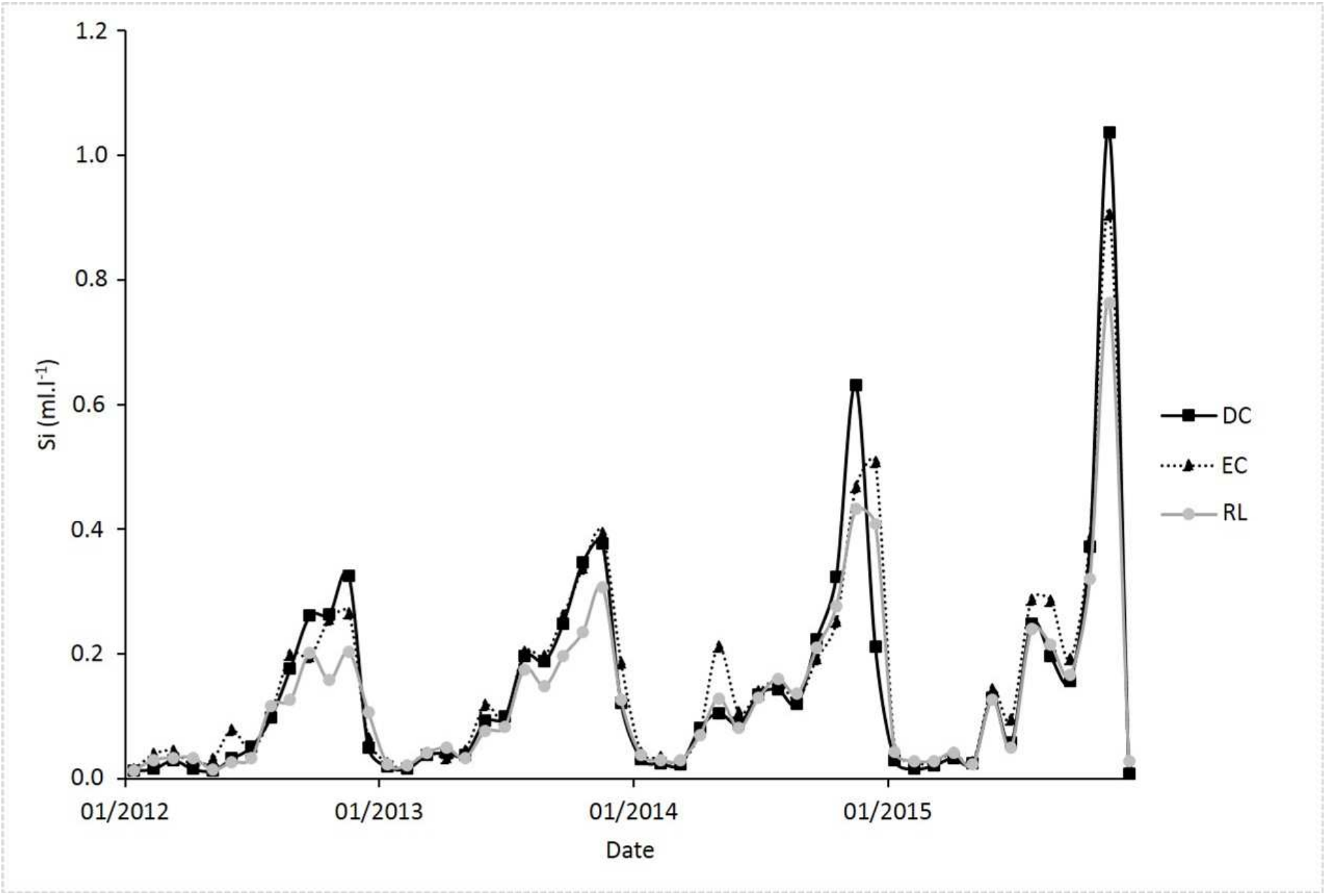
1.2
1.0
0.8
0.6
0.4
0.2
0.0
Si (ml.l-1)
01/2012
01/2013
01/2014
01/2015
Date
DC
EC
RL

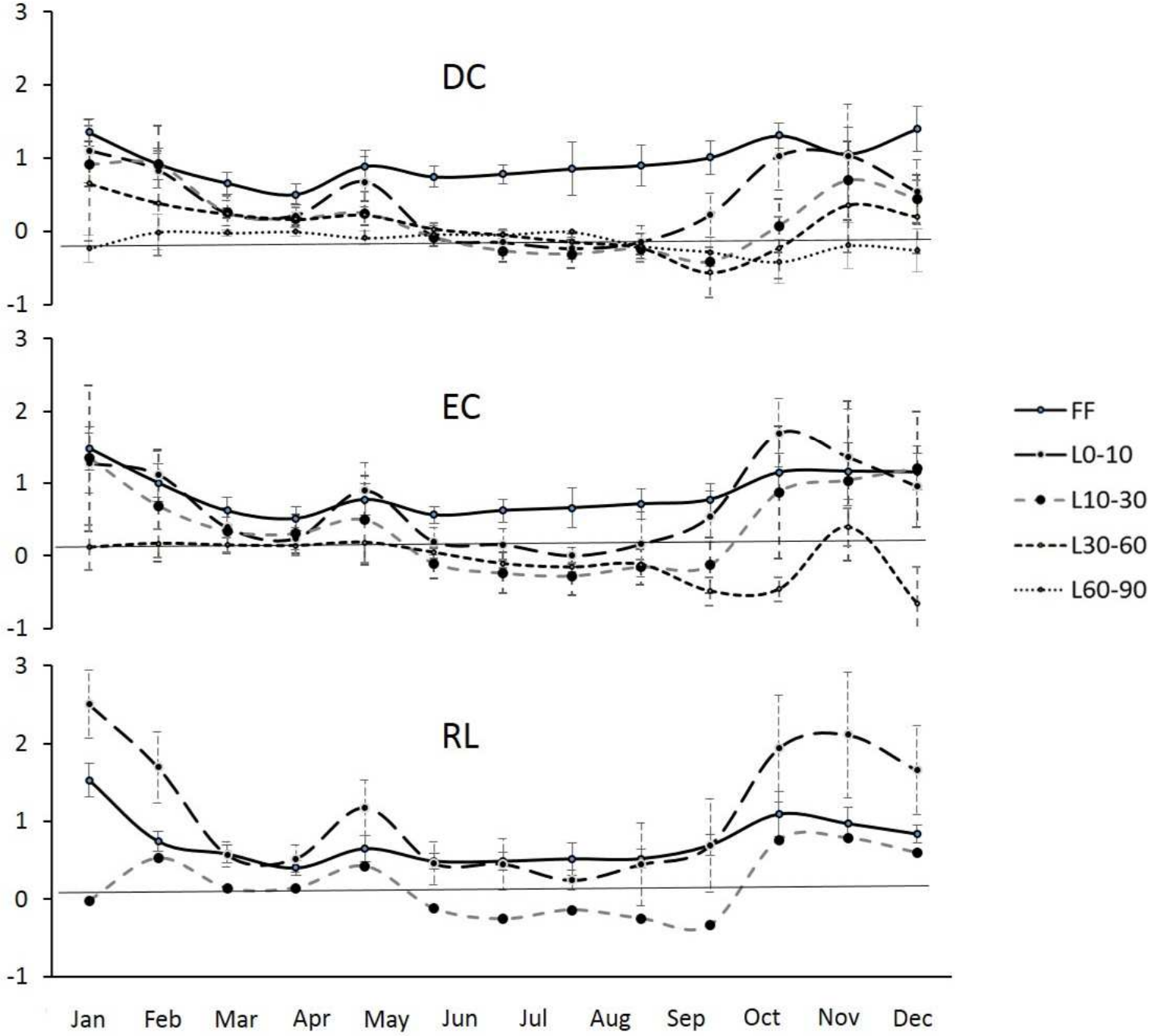
DC
EC
RL
3
2
1
0
-1
Jan
Feb
Mar
Apr
May
Jun
Jul
Aug
Sep
Oct
Nov
Dec
FF
L0-10
L10-30
L30-60
L60-90

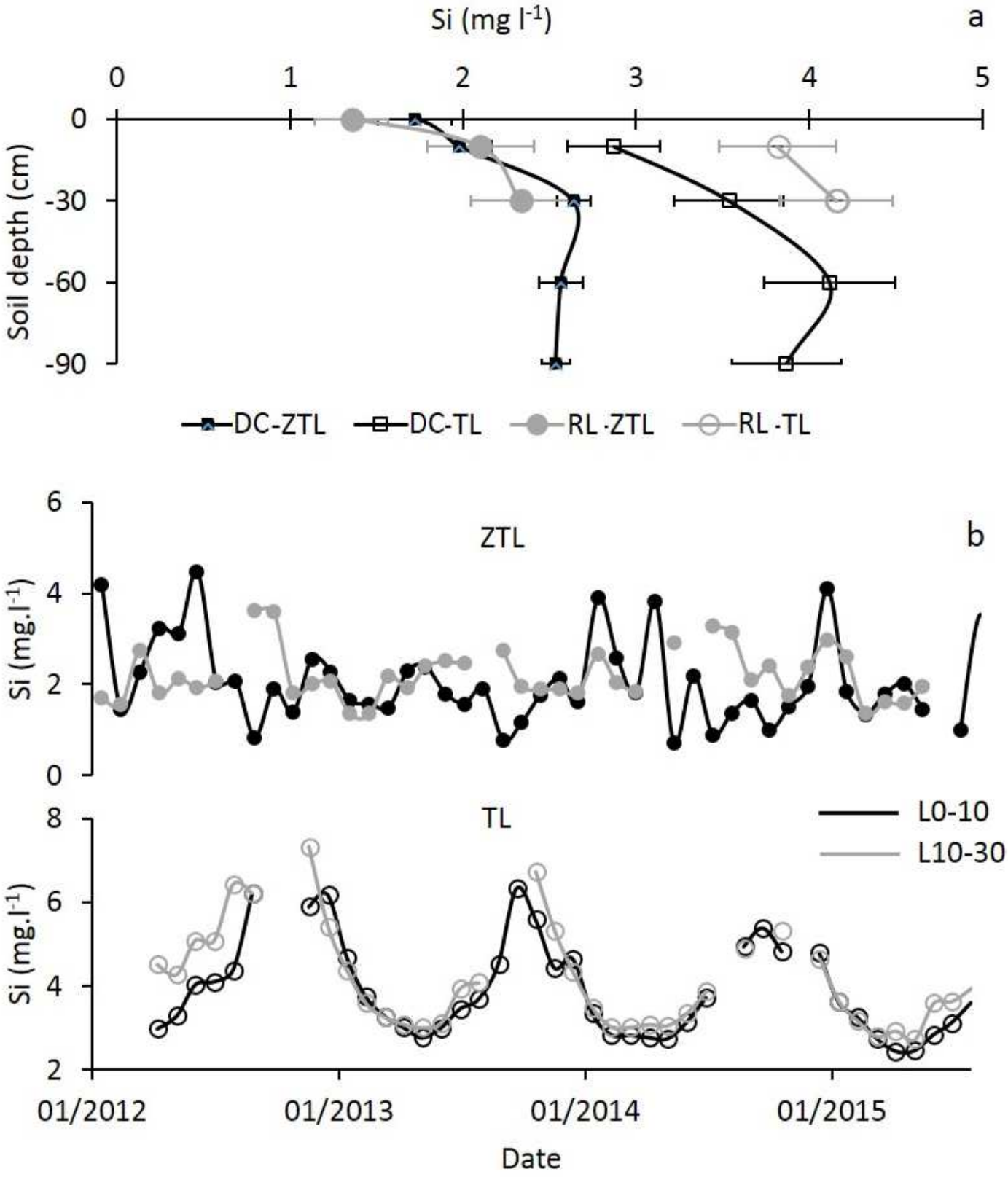
Si (mg l-1)
a
0
1
2
3
4
5
0
-30
-60
-90
Soil depth (cm)
DC-ZTL
DC-TL
RL -ZTL
RL -TL
ZTL
b
6
4
2
0
Si (mg.l-1)
TL
8
6
4
2
Si (mg.l-1)
L0-10
L10-30
01/2012
01/2013
01/2014
01/2015
Date

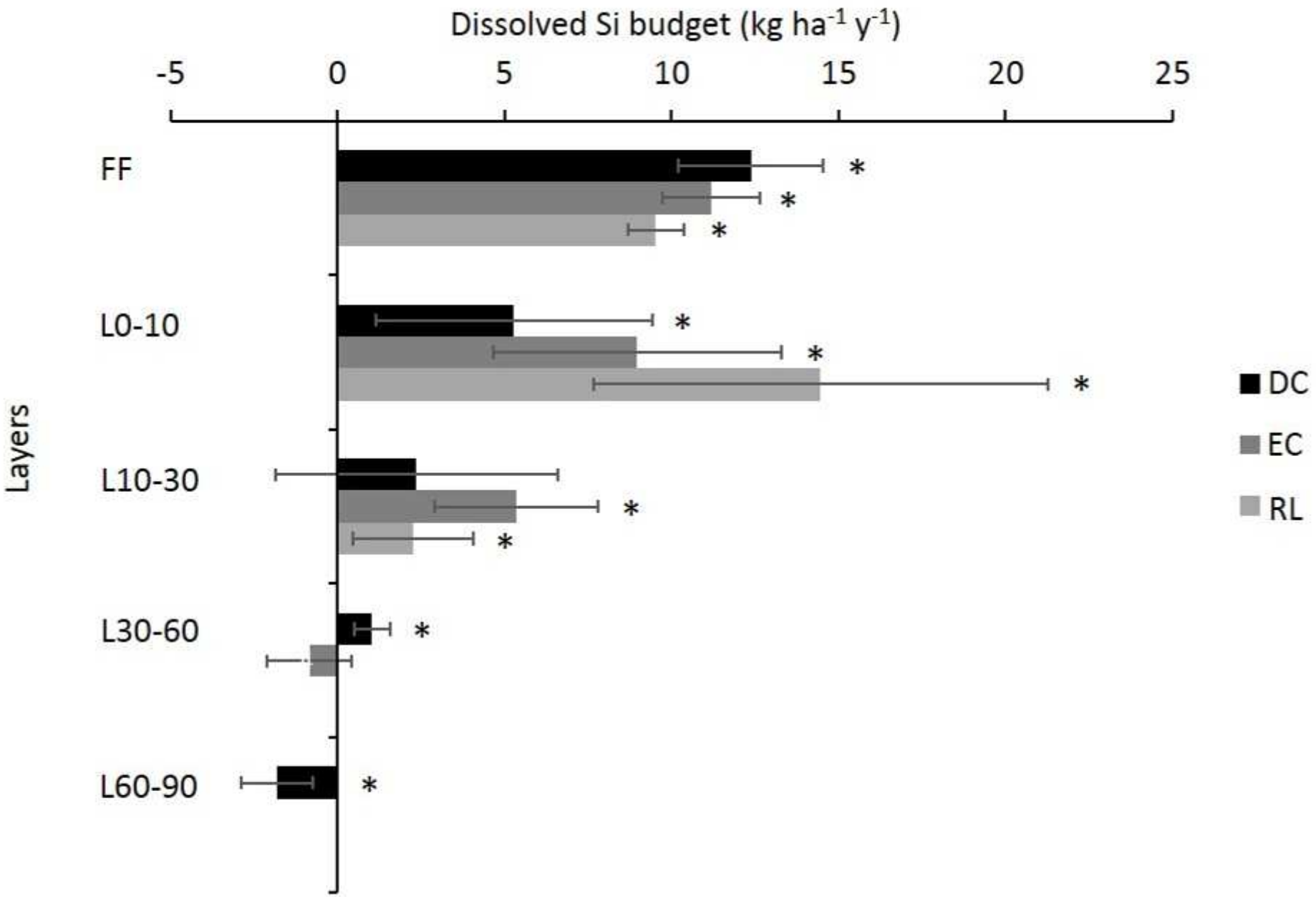
Dissolved Si budget (kg ha-1 y-1)
-5
0
5
10
15
20
25
Layers
FF
L0-10
L10-30
L30-60
L60-90
DC
EC
RL

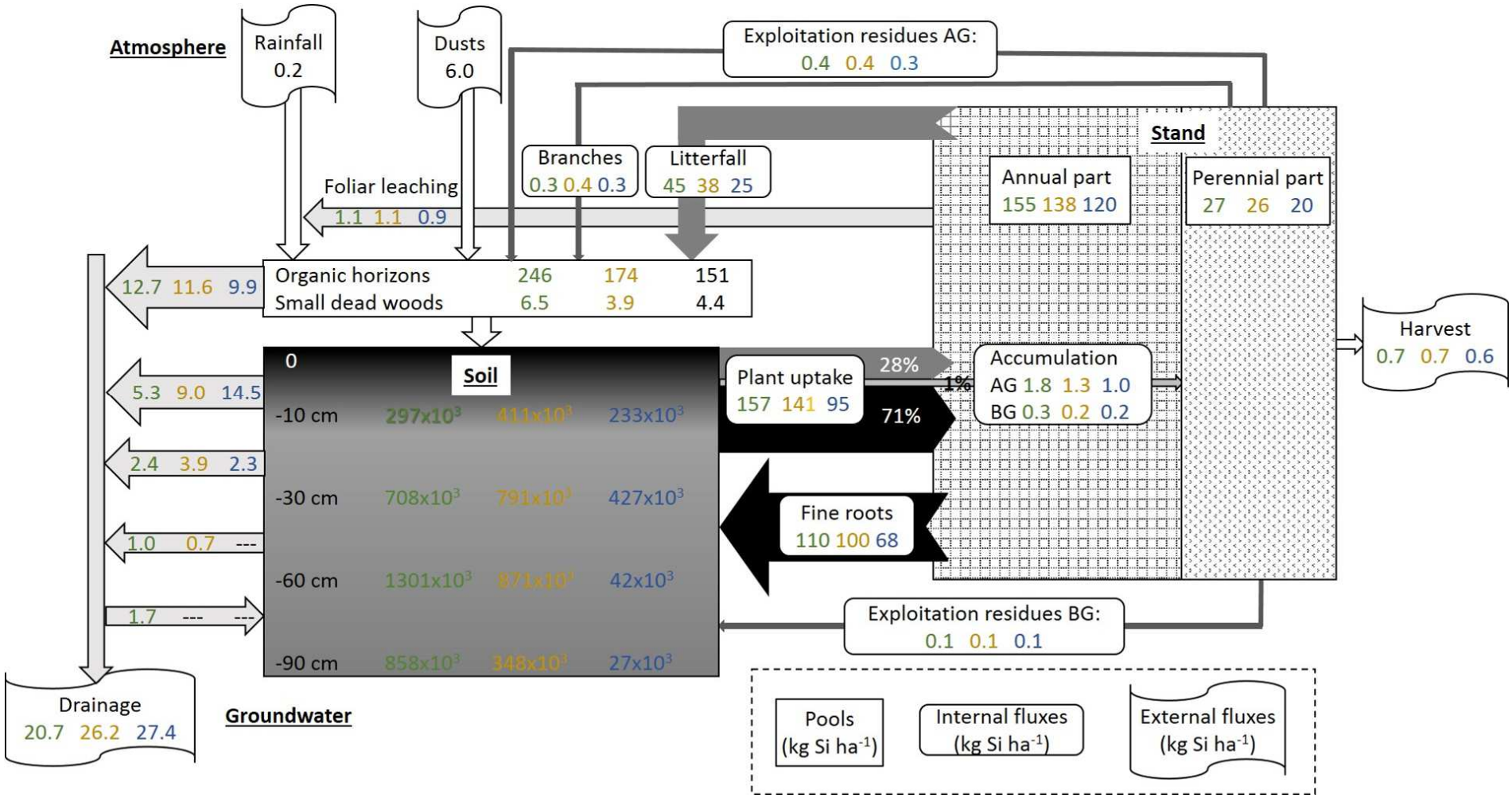
Atmosphere
Rainfall
0.2
Dusts
6.0
Exploitation residues AG:
0.4 0.4 0.3
Stand
Branches
0.3 0.4 0.3
Litterfall
45 38 25
Annual part
155 138 120
Perennial part
27 26 20
Foliar leaching
1.1 1.1 0.9
12.7 11.6 9.9
Organic horizons 246 174 151
Small dead woods 6.5 3.9 4.4
Harvest
0.7 0.7 0.6
0
Soil
28%
1%
71%
Plant uptake
157 141 95
Accumulation
AG 1.8 1.3 1.0
BG 0.3 0.2 0.2
5.3 9.0 14.5
-10 cm
297x10³ 411x10³ 233x10³
2.4 3.9 2.3
-30 cm
708x10³ 791x10³ 427x10³
Fine roots
110 100 68
1.0 0.7 ---
-60 cm
1301x10³ 871x10³ 42x10³
1.7 --- ---
Exploitation residues BG:
0.1 0.1 0.1
-90 cm
858x10³ 348x10³ 27x10³
Drainage
20.7 26.2 27.4
Groundwater
Pools
(kg Si ha-1)
Internal fluxes
(kg Si ha-1)
External fluxes
(kg Si ha-1)

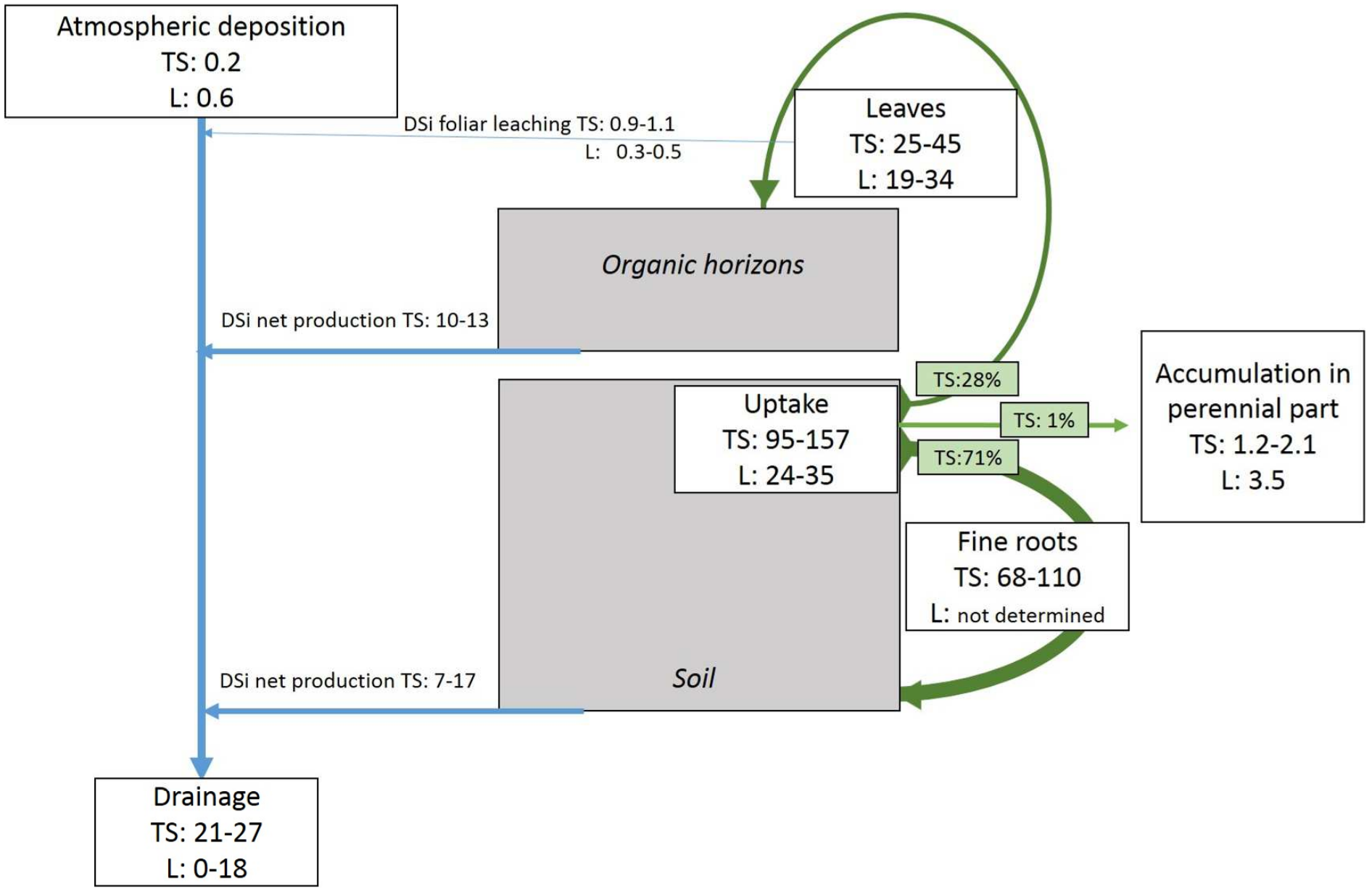
Atmospheric deposition
TS: 0.2
L: 0.6
DSi foliar leaching TS: 0.9-1.1
L: 0.3-0.5
Leaves
TS: 25-45
L: 19-34
Organic horizons
DSi net production TS: 10-13
TS:28%
Uptake
TS: 95-157
L: 24-35
TS: 1%
TS:71%
Accumulation in perennial part
TS: 1.2-2.1
L: 3.5
Fine roots
TS: 68-110
L: not determined
Soil
DSi net production TS: 7-17
Drainage
TS: 21-27
L: 0-18